

# **MSE 320: Machine Design**

## **Fall 2024**

### **Final Report**

Dec 4th, 2024

**Group 5**

XXXXXXXXXXXXXX

Joel Saunders | 301469793

XXXXXXXXXXXXXX

XXXXXXXXXXXXXX

XXXXXXXXXXXXXX

SCHOOL OF MECHATRONIC SYSTEMS ENGINEERING  
SIMON FRASER UNIVERSITY

---

## Table of Contents

<b>Table of Contents</b>	<b>2</b>
<b>Abstract</b>	<b>3</b>
<b>Introduction</b>	<b>4</b>
<b>Ammo-Belt</b>	<b>5</b>
Overview	5
Initial Designs	5
Structural Analysis	7
Final Design	8
Future Improvements	9
<b>Casing</b>	<b>10</b>
Overview	10
Initial Designs	10
Structural Analysis	10
Final Design	14
Future Improvements	14
<b>Motor Drive</b>	<b>15</b>
Overview	15
Initial Designs	15
Structural Analysis	16
Final Design	21
Future Improvements	21
<b>Guide Rail and Blast Door</b>	<b>21</b>
Overview	21
Initial Designs	22
Structural Analysis	22
Final Design	25
Future Improvements	25
<b>Pusher</b>	<b>26</b>
Overview	26
Initial Designs	26
Structural Analysis	28
Future Improvements	32
<b>Full Assembly</b>	<b>34</b>
<b>Conclusion</b>	<b>35</b>
<b>References</b>	<b>36</b>
<b>Appendix: Engineering Drawings</b>	<b>37</b>

## Abstract

This report provides a complete comprehensive overview of the design process made for a tank autoloader system. Substantial strides have been taken to create an efficient, high-capacity and durable system that real modern day battle tanks can benefit from. This report summarizes the development progress made for this project into five main sections: ammo-belt, casing, motor drive, guide rail & blast door, and pusher. Each section outlines critical stages taken, from the initial designs, structural analysis/calculations, modelled parts, and future improvements. The following progress table shown in Table 1 is a breakdown of the completed, active and remaining tasks, alongside their estimated completion dates. All tasks have been successfully completed to the submission date of this report.

*Table 1. Green - Completed; Yellow - Active; Orange - Remaining*

Phase	Description of Work	End Dates
1	Conceptual design	October 3nd
2	Individual part modeling and FEA analysis	Oct 17th (2 weeks)
3	Integrating parts	Oct 31st (2 weeks)
4	Assembly FEA testing and Machine Shop Drawing	Nov 13th (2 weeks)
5	Presentation Preparation	November 25th (12 days)

## Introduction

The design of a tank autoloader system requires addressing multiple complex engineering challenges in a way that balances speed, practicality, and reliability. Due to the multifaceted requirements of this project, the design process was divided into smaller, specialized subsystems. Splitting the autoloader into focused parts, the ammo-belt, casing, motor drive, guide rail and blast door, and pusher. This allowed the team to concentrate on distinct functions within the autoloader. This modular approach speeds up development as it allows for parallel work on each component.

Each subsystem was specified based on unique operational requirements to ensure the autoloader would meet the standards necessary for use in modern armored vehicles.

The shells used are a standard NATO 120mm shell with a 700mm length and a weight of 20kg (*RHEINMETALL – 120MM SMOOTHBORE SYSTEM HOUSE*, n.d.) (increased to 30 kg for a factor of safety). The maximum outer diameter was decided to be 180mm to give room for the rim of the shell.

1. **Ammo-Belt:** The ammo-belt was specified to hold a large load of up to 16-20 rounds, each weighing approximately 30 kg. The belt uses a chain-drive system, selected for its durability and ability to withstand significant weight.
2. **Casing:** The casing had to be designed to store, secure, and transport heavy rounds efficiently within a limited space. A thickness of 3.0mm of belt steel is sufficient to house each unit and resist deformation from the loading.
3. **Motor Drive:** Given the substantial torque required to operate the autoloader reliably, the motor drive needed to deliver precise, high torque at low speeds. The drive system specifications included a 1:2 torque ratio and compatibility with robust sprockets and chains to meet the ammunition load requirements.
4. **Guide Rail and Blast Door:** To protect crew members and ensure smooth round transfer, the blast door had to be capable of withstanding high-stress conditions, with a thick door specified based on safety standards. The guide rail requires minimal deflection, allowing rounds to align precisely with the firing chamber.
5. **Pusher:** The pusher mechanism needed to transfer 30 kg rounds from the ammo belt to the firing chamber with reliability, in any conditions. The pusher needs to go through the ammo belt and blast door and have a maximum extended length of 150cm.

By defining specifications for each part, the team could assess individual design aspects in parallel. This structured approach allows us to efficiently complete this project.

## Ammo-Belt

### Overview

The ammunition belt is an important element in the complete design of the autoloader system. It is designed to efficiently carry 16 rounds, each weighing 30 [kg], and rotate through an input shaft. Each housing for the shells has a diameter of 180 [mm] to fit the standard NATO round of 120 [mm]. The chain must be large enough to withstand and fit the required load. The chain's dimensions were carefully selected and validated with calculations.

### Initial Designs

To begin the process of designing the tank autoloader, it was important to investigate the different types seen in modern day battle tanks, and the driving mechanisms behind them. The autoloader comprises of three main apparatus; the ammunition belt, pusher, and the blast door and rail. Each individual apparatus had to be thoroughly conceptualized to ensure seamless integration of the parts. There were initially two designs considered when designing this component, a drum as well as a chain drive belt.

#### Concept Design 1:

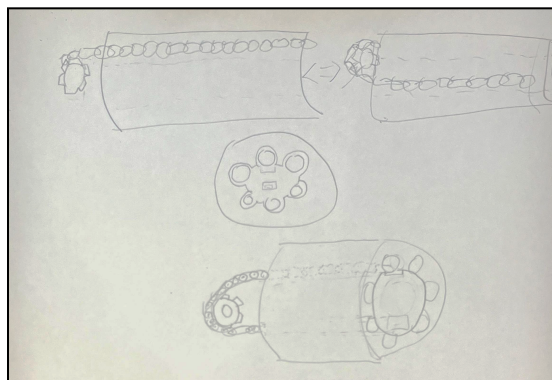


Figure 1.1. Initial sketch of drum loader

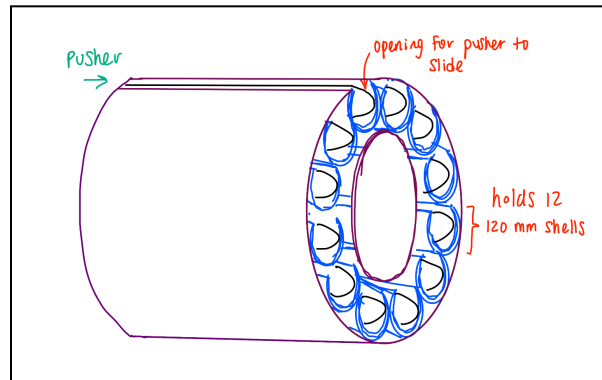


Figure 1.2. Initial sketch of drum loader 2

In the 1st concept, as seen in Figures 1.1 and 1.2, the drum loader is modelled similar to a cylinder of a revolver. The main structure consists of twelve chambers for the rounds. The chambers are designed as open cylindrical casings, when rotated and aligned for loading, the top allows room for the pusher to slide along. The pusher would be fixed at the top and at the back end of the barrel, and would direct the round out of the casing and retract back to its starting position.

Unfortunately, this design occupies a large amount of space due to the drum's massive diameter which ineffectively stores the location of every round. Additionally, the pusher would need to be located at the top which may potentially protrude the surface of the tank. Lastly, due to the large radius, a very high torque would be required to cycle each round through the loader. Due to large volume occupancy, this design was not ideal and was ultimately scrapped and replaced with the ammunition chain belt which is

discussed in the next section. Figure 1.3 shows a CAD model of the initial concept to provide a clearer understanding of the design.

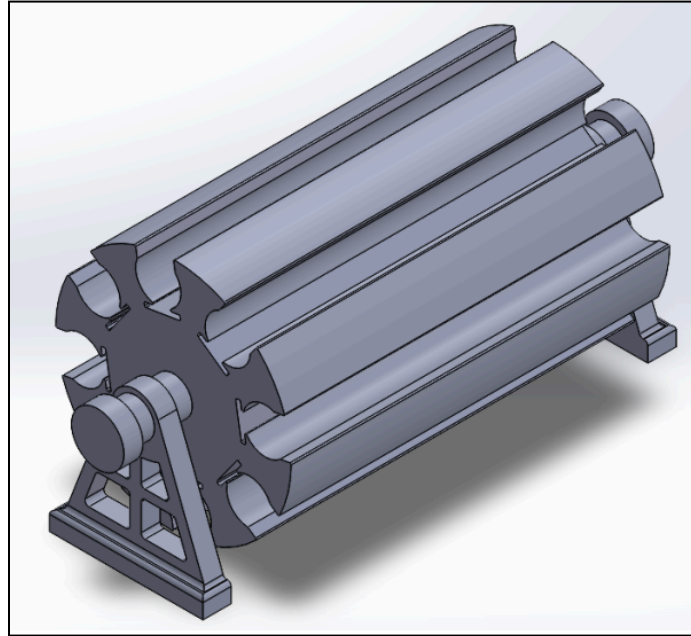


Figure 1.3: CAD model of drum loader

### Concept Design 2:

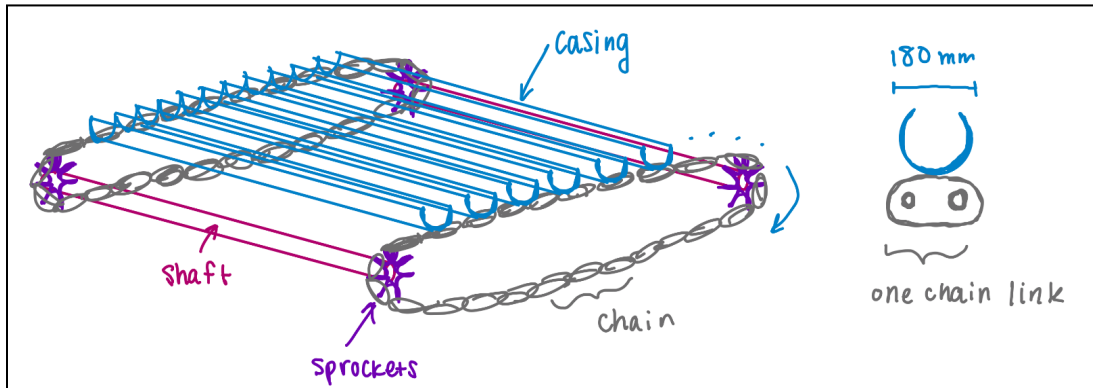


Figure 1.4. Conceptual drawing of chain loader with a unit link shown on the side

This second design shown in Figure 1.4 introduces an entirely different more space-efficient approach, treating the ammunition belt as a conveyor-style system powered by a chain drive. There are two chains, one at the front and rear of the loader. Each is driven by a pair of sprockets that rotate to drive the ammunition into firing position. A motor is also connected to a shaft that transmits torque between the sprockets, which rotates the whole belt. The chain links have a pitch of 4 [in] and are designed to fit a 180 [mm] diameter of one case which carries a single round per link, making it a significantly large chain. However, this is suitable for the design, given there are 16-20 rounds that need to be carried which each

weigh approximately 30 [kg]. Thus a large chain will provide sufficient support and ensure the chain is in tension and not slacking.

## Structural Analysis

Selecting the suitable chain for the ammunition belt:

There are 16 rounds to be carried on the ammunition belt inside casings attached to the chains, which are positioned at the front and rear of the belt. With two chains in the system, there are four sprockets all of equal 30 [cm] diameter. Each shell casing is 180 [mm] in diameter to give room for the rim of the shells as well as to account for any extra material for securing the shells. Given these measurements, the total length of chain needed for one side was first determined using Equation 1.0.

$$L = 2CD + \frac{\pi}{2}(D_1 + D_2) + \frac{(D_1 - D_2)^2}{4CD} \quad (1.0)$$

$$L = 3.94 [m]$$

With the obtained total chain length, the amount of chain meterage per round can be found by dividing by the 16 rounds being carried. This yields 246 [mm] of chain room for each round in its case. This is a suitable distance for each round, as the casings length does not exceed that allowable room. The leftover space allows for the casings to have an adequate distance between each other.

The force downwards on the chain from each shell is computed as follows.

$$F_{shell} = m_{shell}g = (30 \text{ kg})(9.81 \frac{m}{s^2}) = 294 \text{ [N]}$$

Using each shell's force contribution, the total force on the top and bottom of the chain, as well as rounding the sprockets, can be found. Assuming there are 7 rounds on the top and bottom, with one on either side rounding the sprockets.

$$F_{top} = F_{bottom} = F_{shell} * (\# shells) = (294 \text{ N}) * (7 rounds) = 2060 \text{ [N]}$$

$$F_{rounding} = (294 \text{ N}) * (2 rounds) = 588 \text{ [N]}$$

$$F_{tot, down} = 2 * (2060 \text{ N}) + (588 \text{ N}) = 4708 \text{ [N]}$$

Assuming a maximum angle of sag ( $\theta$ ) to be ten degrees downwards on both sides of the chain, the total tension in the chain ( $F_T$ ) can be calculated using trigonometry. Note, the multiple of two is to accommodate the tension experienced on both sides of the chain.

$$F_T = \frac{F_{tot, down}}{2\sin(\theta)}$$

$$F_T = \frac{4708 \text{ N}}{2\sin(10)} = 13.56 \text{ [kN]}$$

Using the total tension in the chain along with more basic trigonometry, the total shaft shear force ( $F_s$ ) is determined.

$$F_s = F_T \cos(\theta) = 13.35 \text{ [kN]}$$

Knowing the total tension in the chain, the shaft shear force, and the dimensions for the ammunition belt casing, the chain suitable for this design is selected. The 64B chain meets all the criteria, as the net tension and shear force fall significantly below the breaking strength of 711.7 [kN]. Additionally, the pitch of the 64B chain is 101.6 mm which fits within the 246 [mm] of chain length allocated to each casing. While the weight from the shells and casings is significantly less than the breaking strength, this chain was selected primarily for its size, to accommodate the casings it carries. Overall, the 64B chain is the preferred choice as its durability can withstand heavy loads and the dynamic movement that comes with being inside a battle tank.

## Final Design

Upon selecting the desired 64B chain, its standard dimensions (*Rollenkette 64B-1 - ELITE*, n.d.) were retrieved and used to construct the rolled and pinned chain links. The final design of the links can be seen in Figures 1.5 and 1.6 respectively. As well, the assembled chain can be seen in Figure 1.7, where the casings and welded plates are expanded upon in the following section.

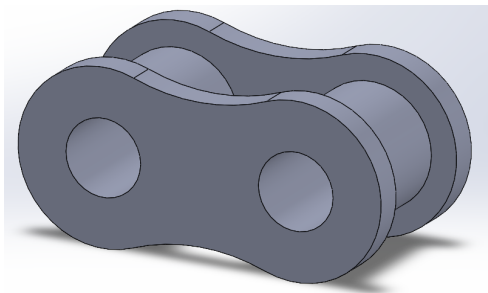


Figure 1.5: Rolled Chain Link

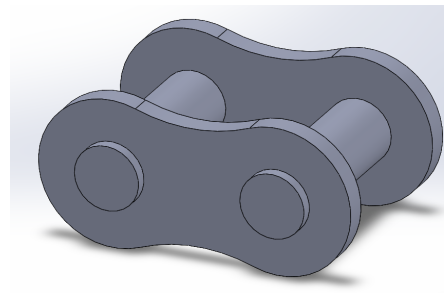


Figure 1.6: Pinned Chain Link

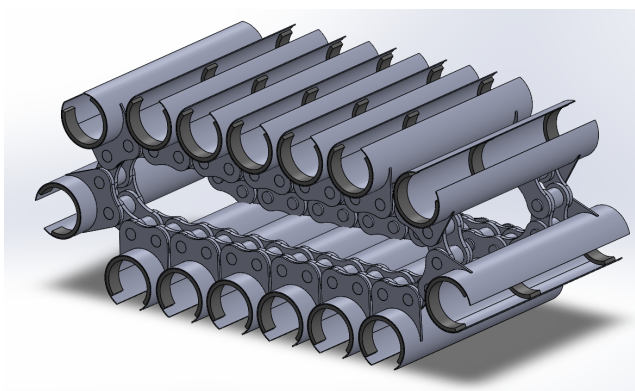


Figure 1.7: Ammo belt

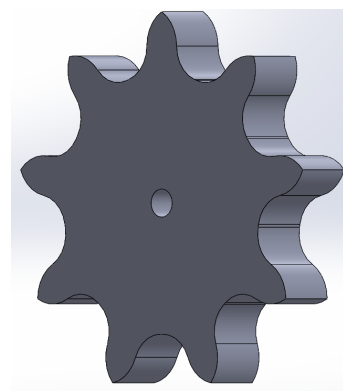


Figure 1.8: Sprocket

---

Given the chain uses standard dimensions, it will be easy to pull off the shelf and order in for the design assembly. However, since this is such a large chain, it was modelled from scratch for the sake of the project and due to the fact it's not commonly used in many applications. Additionally, this design required using a custom made sprocket to suit the dimensions laid out by the chain, shown in Figure 1.8. The sprockets are to be precision-machined and made from steel, where they will be manufactured by a supplier. There are four sprockets connected to two shafts that are driven by a motor and shaft, detailed later. All the drawings for these parts can be found in section one of the appendix.

### Future Improvements

It's important to note a key design change, in that the rolled chain link no longer features an added rim for welding the casing to it. After reevaluating the original design, it became apparent that welding the casings directly to the chain links themselves would be infeasible and an impractical design choice. Therefore, an additional plate, which is discussed in the subsequent section, was designed for the pins of the links to be welded to. In future, it would be ideal to use standard off the shelf sprockets, rather than custom making one for the design. The custom made sprockets tend to come with significantly higher costs as a result of the labor and tooling for the specialized design.

# Casing

## Overview

The design of the casing must be spacious and compatible to carry a variety of ammunition diameters that can be secured and easily cycled around the ammo belt. In this model, a hollow cylindrical shell design was conceived to store the rounds of 120x570mm NATO. The casing has a length of 800mm and diameter of 180mm. It is cut out near the top to allow room for the pusher to pass through as it transfers the round out of the casing and into the firing chamber when being loaded.

## Initial Designs

Some initial designs considered shown in Figure 2.0 is a hollow cylindrical metal plate of 3.0mm thickness. The casing for this design is effectively a rolled sheet of metal with a rectangular footprint of the previously specified dimensions. Having a simple sheet would also ease manufacturability as it involves a simple rolling process. Alternatively, a similar design was also conceived as shown in figure 2.1 where the casing involves an additional flat base where it was proposed to weld on the chain. However this design would not only increase complexity but also increase the weight of the casing which would hinder the performance of the motor shaft; therefore, it was scrapped.

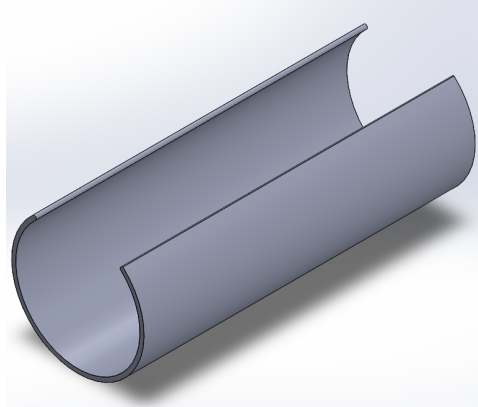


Figure 2.0: Hollow cylindrical casing unit

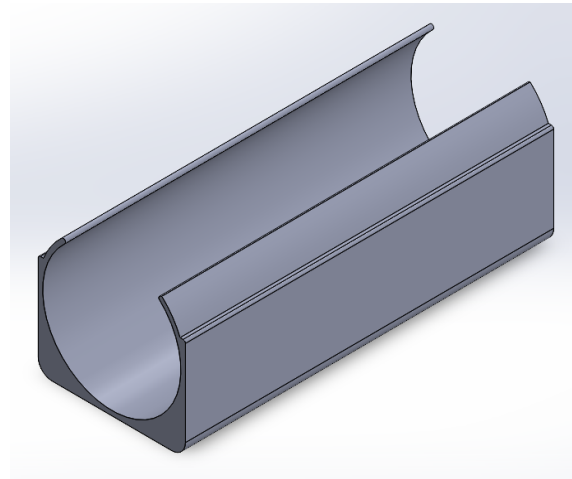


Figure 2.1: Alternative casing design with flat base

## Structural Analysis

Suppose a round is modelled as a cylinder with a uniform mass of 30 [kg]. A casing is of 3.0 [mm] thickness is suitable to support the weight of a round and resist bending while housing the unit. The FEA simulations run under this load are observed in the Figure from the next section below. Using AISI 304 steel, the maximum deflection experienced, in the most extreme case, is 0.07312 [mm] which is roughly 2.5% of the thickness. With the scope of the project, this is an acceptable deformation of 0.0001 [in/in] deformation per length of the casing falling within the 0.00001 to 0.0005 [in/in] range.

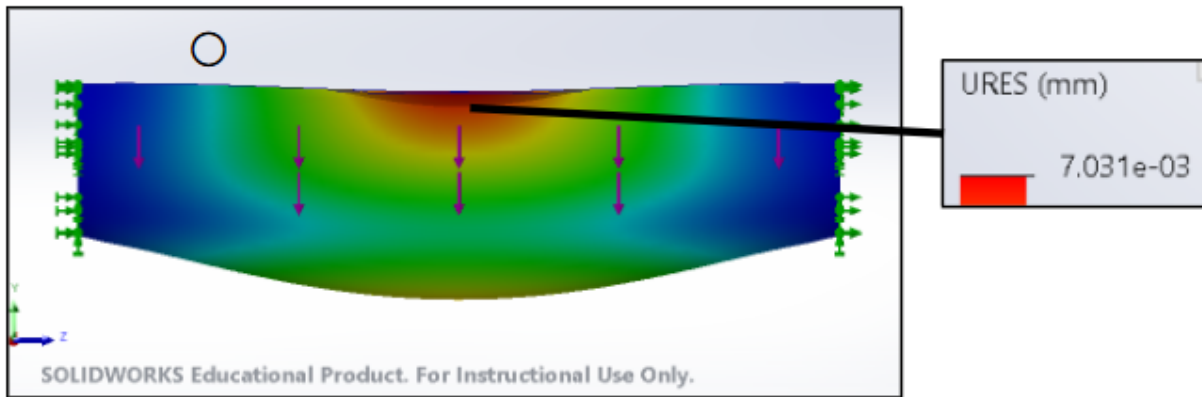


Figure 2.2: FEA results from upright orientation of deflection

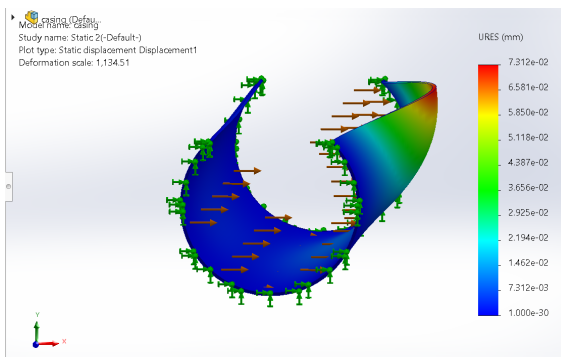


Figure 2.3: FEA results from side orientation of deflection

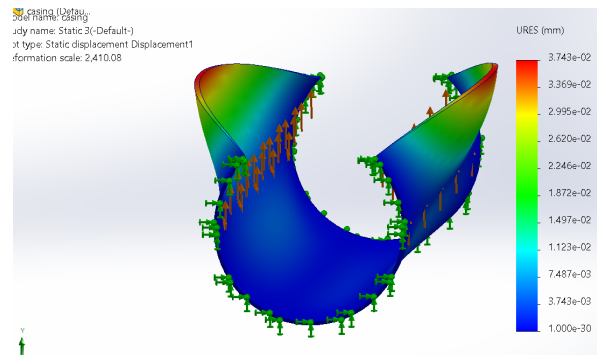
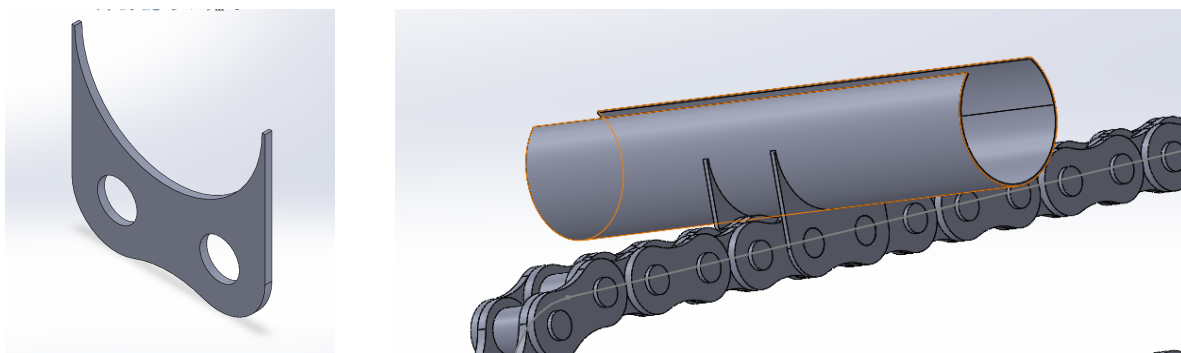


Figure 2.4: FEA results from bottom orientation of deflection

In order to mount the casing with the chain belt system, a separate plate is modeled and welded to each link, seen in Figure 2.5. The plate will consist of holes to allow the chain pins to be welded through, as well as a circular concave top surface to have the casing fit. The plates will be securely fastened with the links and casing will be welded on the top concave surface.



*Figure 2.5: Plate to mate casing with chain*

*Figure 2.6: Assembled view of plate welded to chain*

The following calculations determine a suitable weld joint candidate to securely weld the plate shown in Figure 2.7.

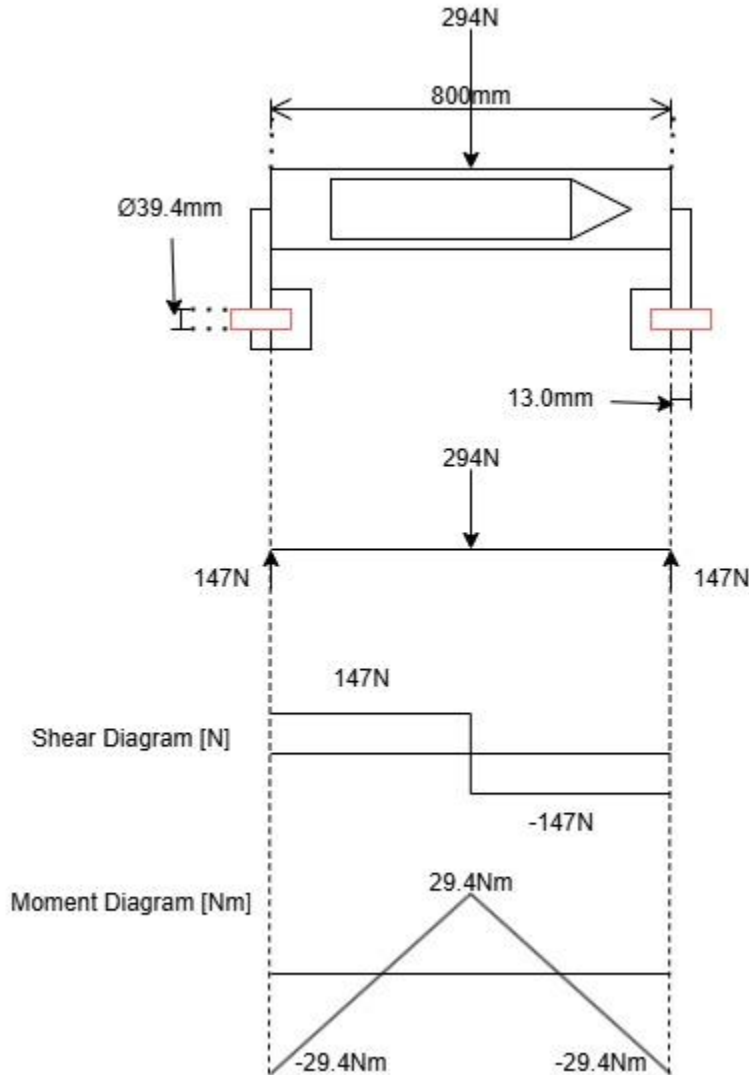


*Figure 2.7: Illustration of beam with shear and moment deflection analysis*

To determine a suitable weld, stress analysis must be done to identify areas under loading. The casing system can be modelled as a straight beam with a point force load at the middle shown previously in Figure 2.7. The distributed load of the ammo shell will be converted to a point force at the middle with a magnitude of 294 [N] (66lb). By applying moment analysis on either ends of the beam, the casing experiences a reaction force of 147 [N] (33lb). Lastly, the moment around the ends and midpoint of the

beam can be determined by computing the equation below. Note: All metric units are converted to imperial in order to select a suitable candidate based on provided data tables.

$$M = \frac{PL}{8} = \frac{(294)(0.8)}{8} = 29.4[Nm] = 260[lbin]$$

Assume the chain link's pins are modelled as individual cylindrical beams with a diameter of 39.4 [mm] (1.55in). The area moment, section modulus, and polar moment are calculated below

$$A_w = \pi(1.55) = 4.87\text{in},$$

$$S_w = \frac{\pi(1.55)^2}{4} = 1.887\text{ in}^2,$$

$$J_w = \frac{\pi(1.55)^3}{4} = 2.925\text{ in}^3$$

respectively.

By performing stress analysis on the pin, there are three main forces that are experienced by the chain: shear force, bending force, and twisting force. Since the casing is fixed to either end of the chain plates, the applied load of 66lb [294 Nm] is halved to evenly share the distributed load. Dividing by the area moment of inertia value will yield the force force length of shear.

$$f_{shear} = \frac{66/2}{4.87} = 6.78[\frac{lb}{in}]$$

Similarly, the bending force per inch is calculated by calculating the moment on either end of the beam. Then dividing by the section modulus will produce the overall value.

$$f_{bend} = \frac{(260)(31.5/2)}{1.887} = 2170[\frac{lb}{in}]$$

Lastly, there is a minor twisting force considered in both horizontal directions.

$$f_{twist,x} = \frac{(66/2)(1.55)(0.5)}{2.925} = 8.74[\frac{lb}{in}]$$

The vertical direction is perpendicular but similar in magnitude.

$$f_{twist,y} = |f_{twist,x}|$$

To account for the contribution of all loadings, the resultant force is computed by applying Pythagorean theorem.

$$f = \sqrt{(8.74)^2 + (8.74 + 2170 + 6.78)^2} = 2186[\frac{lb}{in}]$$

Based on obtained values, the minimum allowable force per inch is 9600 [lb/in], which means the E60 electrode is a suitable candidate to weld the plate to the chain. Additionally, the minimum thickness of the

plate is calculated to be  $\frac{1}{2}$  to  $\frac{3}{4}$  [in] (12.7 to 19.05 [mm]) thickness, which means the plate must have a minimum thickness the same as the side plate in the chain link in order to reduce chances of failure.

Additionally, the casing is lined with stripes of flame-retardant foam of  $\frac{1}{2}$  inch thickness to cushion the rounds as it cycles through the ammo belt which minimizes vibration and internal movement.

## Final Design

The final design of the casing is shown in Figure 2.8 which will be integrated into the overall assembly of the autoloader and operate cohesively with other components.

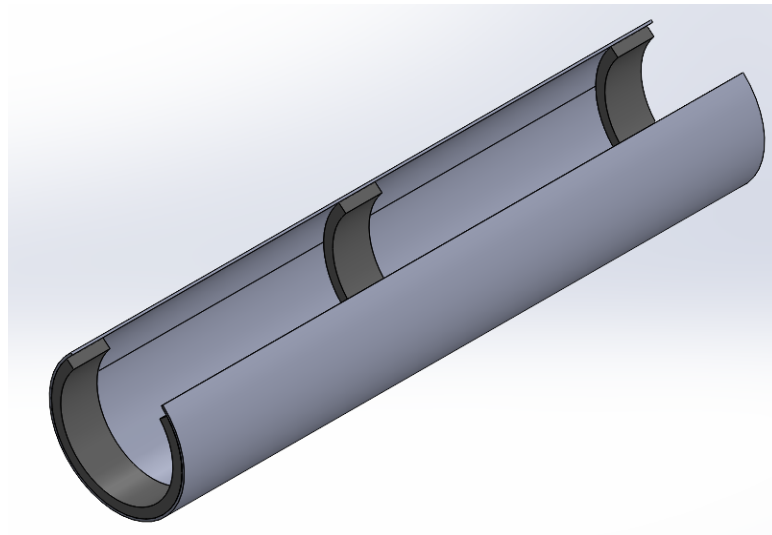


Figure 2.8: Final design of modelled casing with stripes of foam

## Future Improvements

The design of the casing will fit ammunition rounds for the  $120 \times 570$  [mm NATO] ammunition with compatible dimensions of 800mm lengthwise and 180mm in diameter. Elements to further improve upon are finding better methods to secure the rounds with the casing to prevent movement. For example, having an adjustable guide clamp would be necessary to manually secure a type of round in place and minimize movement. Other concepts would involve incorporating spring mechanisms to fasten the plate against one side of the casing wall. Although foam is a suitable temporary substitute, more conceptualization is required to develop a robust solution for a clamp that is both reliable and uniform.

## Motor Drive

### Overview

The motor drive system is designed to power the ammunition belt using a motor, shaft, and chain drive mechanism. The motor is able to provide enough torque, which is transmitted through the shaft and chain, to smoothly rotate the belt.

### Initial Designs

Before concept designs could be considered, a motor selection was required for the power transmission to the autoloader. Motor selection for delivering a sufficient torque to the ammunition system were based on calculations made following the selection of the loader design. Once the belt design had been selected, along with the appropriate sprockets of 30 centimeter pitch diameter, 64B chain, and defining a 16-shell load with an average munition weight of 30 kilograms, the torque required to lift one shell around the sprocket is modelled, and calculated using the torque-force relationship about a radius.

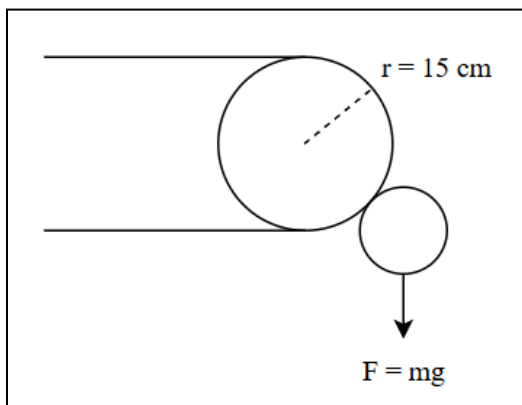


Figure 3.0: System Model for Torque Calculation

The calculations are as follows.

$$T = Fr$$

$$T = (9.81)(30)(0.15) = 44.145[Nm]$$

where T is torque [Nm], F is force [N], and r is sprocket radius [m].

Assuming that the loader may need to move a maximum of two shells at a time, the torque calculated in Equation 3.0 is multiplied by two, resulting in a value of 88.29 Newton-meters of torque required. Given the heavy-duty application of the autoloader design, and that the system's chain speed would be low, hydraulic motor 6299K53 was selected the motor supplies a maximum torque of 208.118 Newton-meters, and with a safety factor of 2 applied, desired torque to be delivered becomes 416 Newton-meters. With the design torque defined, power transmission designs can be made.

## Concept Design 1

The first concept design for power transmission was a gear system. This system would entail attaching a gear to the motor, with a larger gear attached directly to the shaft of the 64B chain drive. This gear system would deliver a 1:2 torque ratio to the ammo belt, which would be sufficient in moving the load and accounting for any losses related to friction or tension in the belt chain.

This design was abandoned due to the complications in keeping the gears lubricated, and concerns with gears failing due to the immense torque being transmitted through the gears.

## Concept Design 2

The second concept design delivers power to the ammo belt using a chain drive, with a similar 1:2 ratio as seen in the first concept design. A smaller sprocket would attach to the 6299K53 motor, and link to a larger sprocket with a chain link. Calculations for center distance and chain length would be required, but made simple as pitch diameters and number of teeth would be provided by a manufacturer based on sprocket selection.

This design was selected for the power transmission of the motor drive system, as lubrication would be easier than the gear system, and the chain drive would be more effective in handling the large torque to be transmitted to the ammo belt. With this decision made, selections and calculations were to be completed for the remainder of the design process.

## Structural Analysis

With the chain concept selected, desired sprocket selections can be made. It was important to choose large sprockets with high teeth counts in order to have decisions that are compatible with stronger chains, such as a 10B chain or larger; these chains exhibit high break strengths, which are needed to handle the power transmission. Additionally, the larger size makes them less susceptible to friction losses as the system is operating.

Safety Factor = 2 Motor Torque We want to deliver 2x torque to account for losses														
Diameter/Force		Potential Driving Sprocket			Potential Driven Sprocket			Potential Chain			Remarks			
Torque (Nm)	Diameter (m)	Force (N)	Teeth	Pitch (mm)	Diameter (m)	Teeth	Pitch (mm)	Diameter (m)	Chain	Break Strength (N)	Result	Notes	Shaft Dia.	Selection
416	0.01	83200	9	25.4	0.07427	36	25.4	0.29143	16B	42300	Pass	B-Hub	1"	12B23 and 12B46
	0.02	41600	9	25.4	0.07427	18	25.4	0.14627	16B	42300	Pass	B-Hub		
	0.03	27733.3	10	25.4	0.0822	20	25.4	0.16237	16B	42300	Pass	Tapered Bushed		
	0.04	20800	14	25.4	0.11415	28	25.4	0.22686	16B	42300	Pass	B-Hub		
	0.05	16640	14	19.05	0.08561	28	19.05	0.17014	12B	28900	Pass	B-Hub		
	0.06	13866.7	23	19.05	0.1399	46	19.05	0.27915	12B	28900	Pass	B-Hub		
	0.07	11885.7	24	19.05	0.14595	48	19.05	0.29127	12B	28900	Pass	B-Hub		

Figure 3.1: Sprocket Selection Spreadsheet

Sprockets selected were the 12B23 and 12B46 B-hub sprockets from USA Roller Chain. The B-hub design for a 19.05-millimeter pitch for these sprockets have hub diameters of 100-millimeters and 107-millimeters, tooth width of 11-millimeters, and a length through bore of 40-millimeters. These

sprockets have pitch diameters of 139.9-millimeters and 279.15-millimeters respectively, making them satisfactory choices for withstanding applied torque and minimizing friction losses. These sprockets have a 19.05-millimeter pitch, making them compatible with the 6027K199 12B chain from McMaster Carr, exhibiting a 28900-Newton breaking strength and 6672-Newton working load, making it an excellent choice for the motor drive. The 23:46 tooth ratio results in the required 1:2 torque ratio.

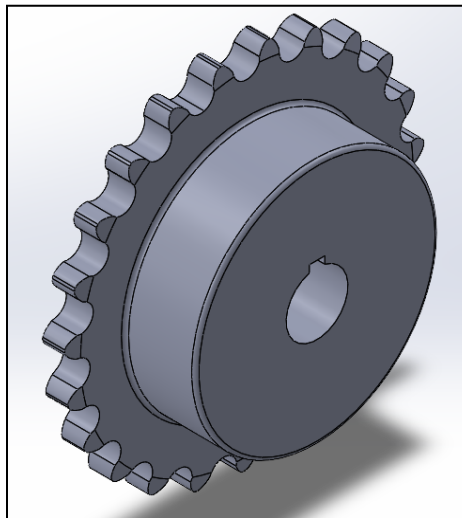


Figure 3.2: 12B23 Sprocket

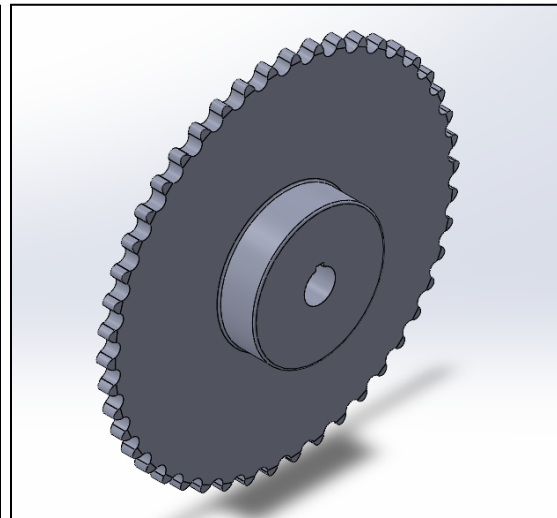


Figure 3.3: 12B46 Sprocket



Figure 3.4: 6027K199 12B Roller Chain [1 ft]

With the chain and sprockets selected, center distances, chain length, and angles of wrap around each sprocket are desired. Selecting an initial center distance of 30-pitches, angle of wrap around each sprocket and chain length in pitches are calculated.

$$\theta_1 = 180 - 2\sin^{-1}\left(\frac{N2-N1}{2*CD}\right)$$

$\theta_1$  is the angle of wrap around the smaller sprocket [deg], N2 is the teeth around the larger gear, N1 is the teeth around the smaller gear, and CD is the center distance [pitches].

$$\theta_2 = 180 + 2\sin^{-1}\left(\frac{N2-N1}{2*CD}\right)$$

$\theta_2$  is the angle of wrap around the smaller sprocket [deg].

$$L_c = 2 * CD + \frac{N2+N1}{2} + \frac{(N2-N1)^2}{4\pi^2 CD}$$

$L_c$  is the length of the chain [pitches].

From these calculations, the angles of wrap are 134.9-degrees and 225.1-degrees, and the chain length is 94.95-pitches, or 1808.7-millimeters. This chain length is increased to 1828-millimeters, as it translates to a flat 6-feet, which is the closest chain length that can be ordered from McMaster-Carr. This length is equal to 96-pitches, and the center distance is recalculated.

$$CD = 0.25(L_c - \frac{N2+N1}{2} + \sqrt{[L_c - \frac{N2+N1}{2}]^2 - \frac{8(N2-N1)^2}{4\pi^2}})$$

The new center distance is 30.5306-pitches, or 581.608-millimeters. With these calculations complete, the size of the sprockets, distance between sprockets, and chain length have been determined, and the chain design process is complete. With the completed chain design, a shaft is required to transmit the power from the motor drive to the rest of the autoloader system.

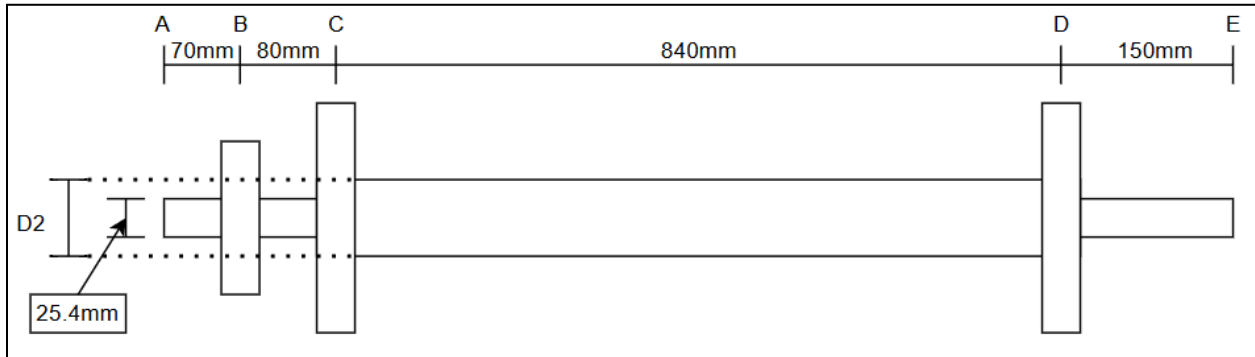


Figure 3.5: Driven Shaft Analytical Model

The diameter D2 must be carefully selected such that the shaft can withstand the torque applied, as well as not deflect too much; significant deflection would cause the casings to be slanted as the loader operates, which is not ideal. In order to determine the diameter in the shaft, the moment at point C is required.

Knowing that the 416-Nm torque is applied through the B46 sprocket at point B, and assuming half the torque is shared between points C and D, sprocket force calculations are as follows:

$$(PD_{B46} - PD_{B23}) * 0.5 = 69.625$$

$$\theta_B = \tan^{-1}(69.625/CD_{mm}) = 6.83^\circ$$

$$F_B = \frac{T_B}{PD_B * 0.5} = 2980.5 N$$

$$F_{BX} = F_B \cos \theta_B = 2959.3 N, F_{BY} = F_B \sin \theta_B = 354.5 N$$

$$F_C = F_D = \frac{T_B * 0.5}{PD_C * 0.5} = 1386.7 N$$

As the sprockets on C and D are a 1:1 ratio, there is no angle, thus the forces acting on the x-plane are equal to the magnitude of force acting at each point, and the forces acting on the y-plane are zero.

Summing the moments in each plane at point A and taking a sum of the forces in the x and y planes yields the following reaction forces:

$$F_{EX} = 1568.4 \text{ N}, F_{AX} = 4164 \text{ N}$$

$$F_{EY} = 21.8 \text{ N}, F_{AY} = 333 \text{ N}$$

The calculated forces yield the following shear and moment diagrams:

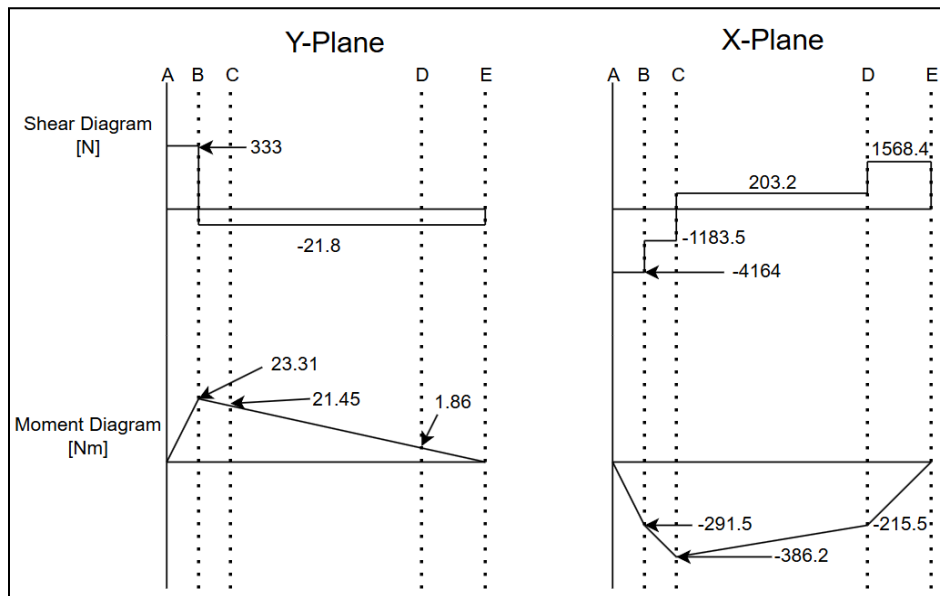


Figure 3.6: Driven Shaft Shear and Moment Diagrams

The y-plane and x-plane moments at point C are 21.45 and -386.2, in Newton-meters. The resultant moment is calculated to be 386.8 [Nm]. The selected material is AISI 304 steel, which exhibits a yield strength of 215 MPa and a tensile strength of 505 MPa; the resulting endurance limit is 197 MPa.

Assuming a stress concentration factor of 2.5 from a sharp fillet on the shaft, a design factor of 2, a reliability factor of 0.81, a size factor of 0.9, and a material and type-of-stress factor of 1, the actual endurance limit is calculated:

$$s'_n = 197(0.81)(0.9) = 143.6 \text{ MPa}$$

With the actual endurance limit and the required moment, the larger diameter of the shaft can be calculated:

$$D_2 = \sqrt{\frac{32*2}{\pi} * \sqrt{\left[\frac{2.5*386.8}{143600}\right]^2 + \frac{3}{4} \left[\frac{416}{215000}\right]^2}} = 52.1 \text{ mm}$$

Solving for torsional deformation across the 0.84-meter long section of the shaft:

$$\theta = \frac{416*0.84*32}{200*10^9*0.0521^4\pi} = 0.00242 \text{ rad} = 0.139^\circ$$

Knowing that the circumference of the large section of the shaft is 327.35-mm, and 0.139 degrees is 0.0386% of a full rotation, shaft deflection is estimated to be 0.46-mm. With the theoretical shaft design complete, the model is created:

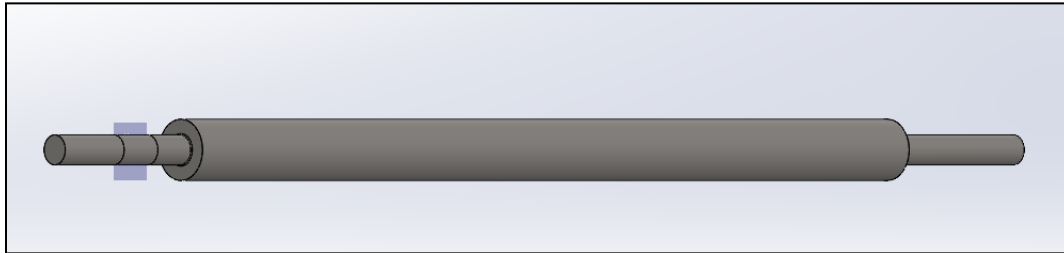


*Figure 3.7: Driven Shaft SolidWorks Model*

In order to better understand the deflection caused by the 416-Nm torque, a static study is conducted, and the results are compared to the calculations:

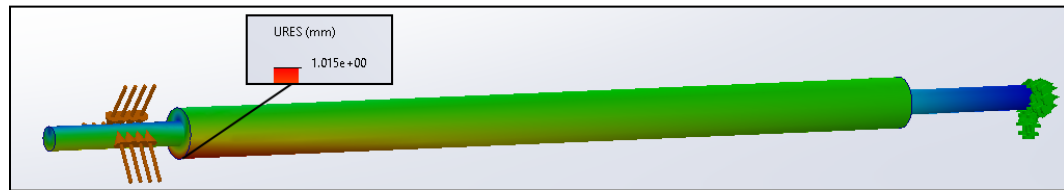


*Figure 3.8: Driven Shaft SolidWorks Study*

From this study, a maximum deflection of 1.015-mm is observed, a 2.2-times increase from the calculated value. The observed deflection is taken to account for the deflection in degrees per inch of length:

$$\text{Deg}/\text{Inch} = (1.015 * 10^{-3})(\frac{180\text{deg}}{\pi})(\frac{1}{840\text{mm}})(\frac{25.4\text{mm}}{1\text{inch}}) = 0.00176$$

This metric falls within the range of 0.001-0.01, which deems the deflection of the shaft to be acceptable for a general machined part. Each component is then ready to be put together, with a final assembly including the motor, the set of sprockets, the chain, and the shaft. The shaft rests in the walls of the loader with 1-inch precision needle-roller bearings. The motor receives an additional plate mount, made of AISI 304 steel, which attaches to the motor with two half-inch screws; the plate itself attaches to the wall of the autoloader with four three-quarter inch screws, where all screws are grade A325 steel. With the shaft design complete, the power transmission design is finalized, and this component is ready to be adapted to the full autoloader design.

## Final Design

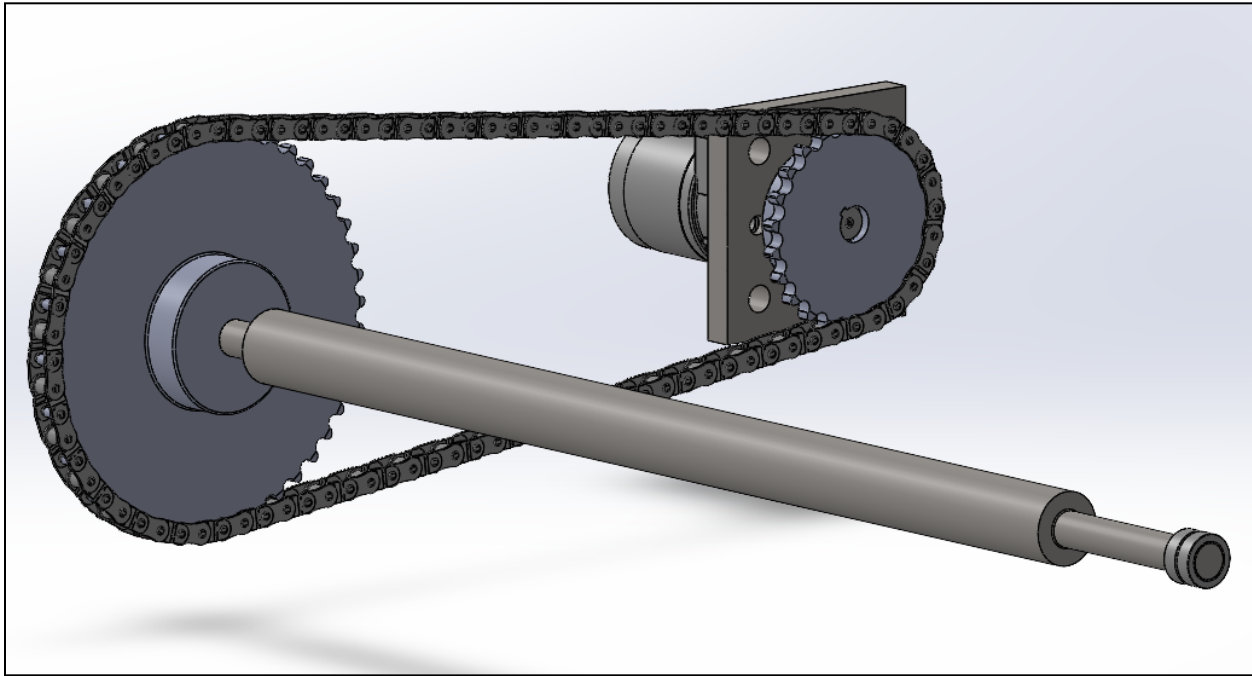


Figure 3.9: Power Transmission Final Design

## Future Improvements

Future improvements consist of major design changes, which would require a significant portion of time in the development process; investigating the performance of the system by swapping the chain for a gear train would be notable if it works, as this would significantly reduce the amount of moving parts and complexity of the power transmission system. Additionally, investigating the effect of changing the bore of the sprocket set to allow a larger initial diameter for the shaft could prove useful in minimizing the deflection endured by the shaft from the applied torque. Furthermore, if a prototype were created, testing of a 416-Nm torque is necessary would be done, possibly allowing for a reduced torque to be put in place, which would also minimize the deflection in the shaft.

## Guide Rail and Blast Door

### Overview

The blast door and ammo rail were put together in the design process due to their similarity and proximity.

The blast door is a thick steel door that is intended to protect the occupants of the vehicle in the event that the ammunition detonates. The door needs to be able to open during the loading procedure and be closed otherwise. The ammo rail supports the shell while it is being pushed from the ammo belt to the chamber. The ammo rail also moves out of the way of the recoil of the chamber to ensure the rail is not damaged.

## Initial Designs

Two conceptual designs were made to attempt to find the best solution to the design problem.

### Concept Design 1:

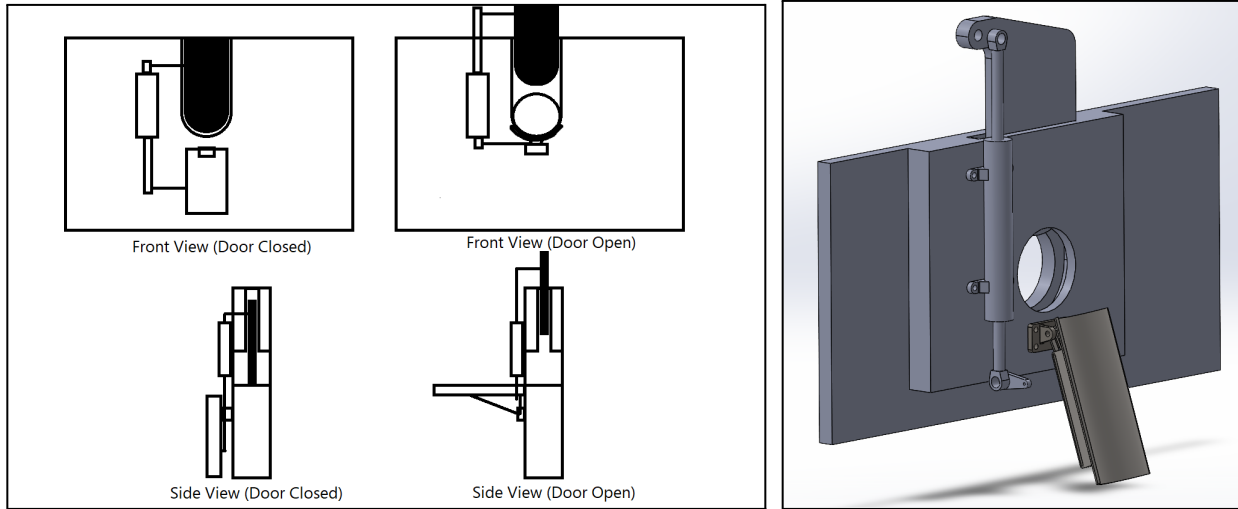


Figure 4.1, Single Hydraulic Cylinder Design

Figure 4.2, Single Hydraulic Cylinder Design Model

### Concept Design 2:

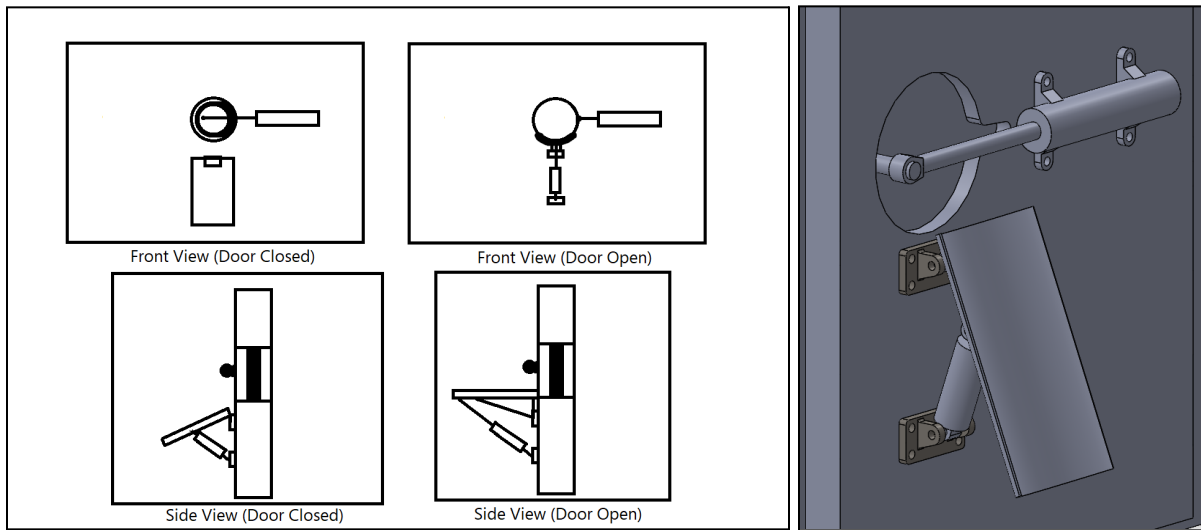


Figure 4.3, Double Hydraulic Cylinder Design

Figure 4.4, Double Hydraulic Cylinder Design Model

Conceptual design 1 (Figure 4.1 & 4.2) was intended to reduce complexity by only needing one hydraulic cylinder but ended up increasing complexity with the linkages needed to connect the rail as well as the eccentric loading on the door could cause jamming. It was decided to use two hydraulic cylinders as seen in conceptual design 2 (Figure 4.3 & 4.4) to decrease complexity.

## Structural Analysis

The entire rail assembly was simulated to ensure the complexities introduced to the system by the number of parts were accounted for. The hydraulic cylinder was not included due to the limitations of solidworks. A component interaction was used with an interaction type “contact” to simulate the interaction between

the hinges and the rail. A maximum deflection of 0.57 [mm] and a stress far below the yield strength of the material was found and was decided to be acceptable.

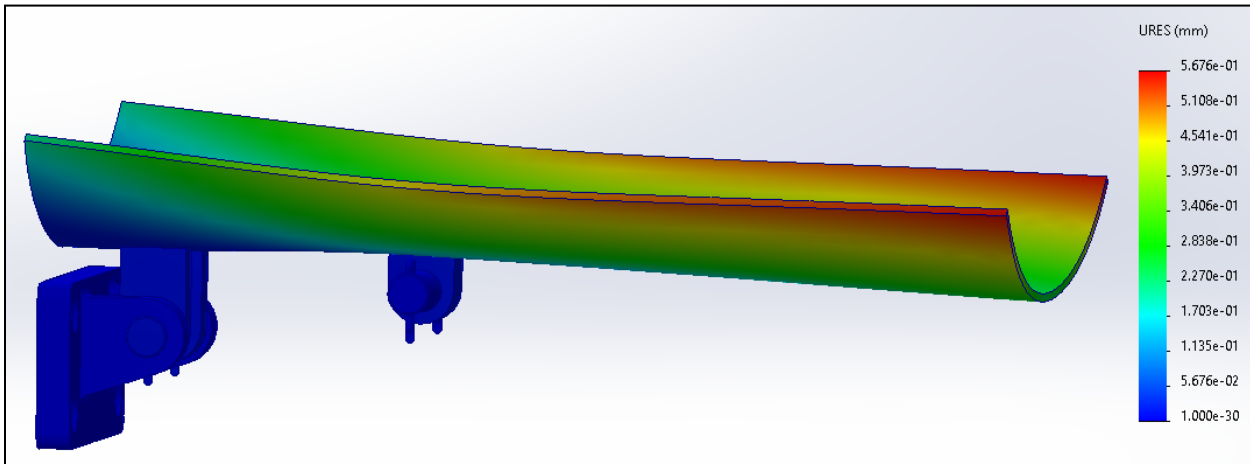


Figure 4.5, Rail Deflection FEA

This rail will be made by rolling a 2.5 [mm] steel into a 18 [cm] radius circle. The connections to the hinge and hydraulic will be machined and welded to the rail.

The blast door's thickness was considered as this is a critical part for crew safety, the blast door separates the volatile ammunition from the crew. The blast door must be thick enough to survive a detonation of the ammunition so the M1A1 Abrams's similar blast door thickness of 28.6 [mm] was used as a comparison (*M1A2 Main Battle Tank Firing Main Gun - Interior View*, n.d.). A 30 [mm] blast door was used in our design. The weight of the door is a consideration as it weighs ~18 kg and it is intended to slide on its side during the opening and closing procedure, so friction must be considered. Strips of PTFE, a low friction plastic, are fixed to sliding surfaces to reduce the friction coefficient to 0.2 (*Coefficient of Friction Reference Chart*, n.d.). PTFE strips were placed on all sliding surfaces of the blast door and screwed into place using countersunk screws to ensure the sliding surface is flush.

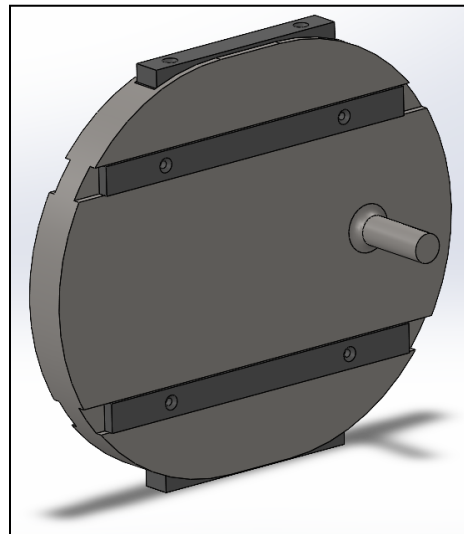


Figure 4.6, Blast Door

The piece that connects the door to the hydraulic is a 2 [cm] diameter rod and is welded onto the door with a  $\frac{1}{4}$ " leg size to support the large bending forces applied.

With a coefficient of friction of 0.2 and a weight of 19 [kg] a frictional force can be found of 37.2 [N]. It can be assumed that a large frictional force will be imparted on this door as it is pushed eccentrically by the hydraulic piston so it is important to overspec. The piston that was selected was 1524N114 1  $\frac{1}{2}$ " bore diameter and 8" stroke with a maximum force of 20000 [N]. This piston was selected because it was the smallest available with an 8" stroke which was needed for this application as well as its force being far above what is required. An estimated worst case scenario is the door requiring 250 [N] of force to open. A simulation was done to test the factor of safety in this scenario (Figure 3G). A factor of safety of 10 was found in the simulation.

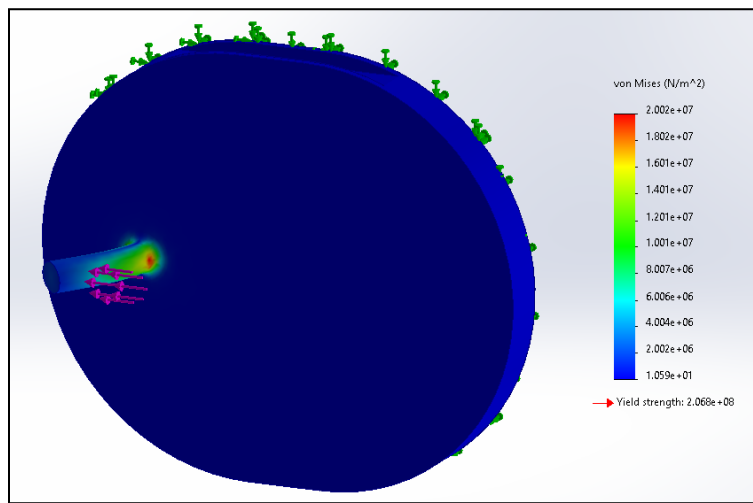


Figure 4.7, Blast Door FEA

Due to the limitations of Solidworks abilities in simulating the mechanics of welds an analytical computation was done (Mott et al., 2017). An E60 electrode and leg size of  $\frac{1}{4}$ " was used.

$$\text{Moment on weld} = 56.2 \text{ lb} * 2.36 \text{ [in]} = 132.6 \text{ [in lb]}$$

$$S_w = \pi(d^2/4) = \pi((0.787 \text{ [in]})^2/4) = 0.486$$

$$\text{Force per inch of weld} = M/S_w = 132.6/0.486 = 272.8 \text{ [lb/in]}$$

$$\text{Shear on weld} = 56.2 \text{ [lb]}$$

$$A_w = \pi d = \pi * 0.787 = 2.47$$

$$\text{Force per inch of weld} = V/A_w = 56.2 \text{ [lb]}/2.47 = 22.75 \text{ [lb/in]}$$

$$\text{Total force per inch of weld} = 285.6 \text{ [lb/in]}$$

$$\text{Allowable force per inch of weld} = 9600 * 0.25 = 2400 \text{ [lb/in]}$$

Given these calculations the factor of safety of these welds is  $\sim 8.4$ . This is satisfactory for our application.

## Final Design

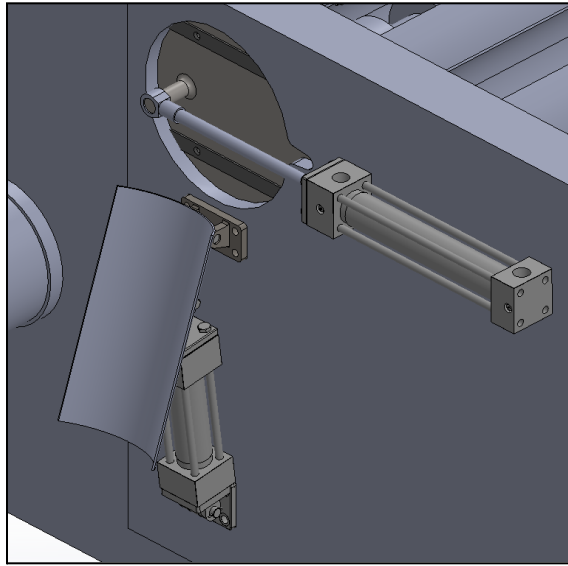


Figure 4.8, Blast Door and Rail Closed

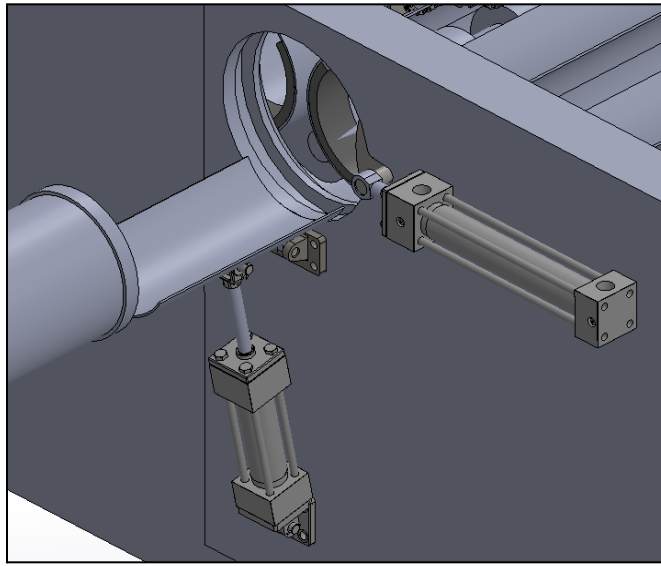


Figure 4.9, Blast Door and Rail Open

The final design for the blast door and ammo rail combines the insights and lessons learned from the initial conceptual designs and structural analysis. The blast door and ammo rail have been integrated into a single system. The blast door is mounted on a cast frame, casted at the same time as the entire turret and machined down to tolerance. This design eliminates the complexities of linkages seen in Concept Design 1, and ensures that the blast door moves efficiently without the risk of jamming.

The blast door is made from 30 [mm] thick steel, ensuring that it can withstand the explosive forces from ammunition detonation. The PTFE strips are used to reduce sliding friction and are securely fastened with countersunk screws.

Both systems use hydraulic cylinders as in a tank there is already a hydraulic system and because both mechanisms need linear actuation.

Overall, the final design for the blast door and ammo rail system offers a balance of safety, functionality, and ease of maintenance, ensuring that the system can operate effectively in a tank autoloader while protecting the crew in the event of an ammunition detonation.

All drawings and parts used can be found in the appendix.

## Future Improvements

Improvements to the system could be finding smaller hydraulic cylinders that more closely supply the force needed. Currently the cylinders supply ~80 times more force than is needed resulting in additional bulk and weight. The pin connecting the blast door to the hydraulic cylinder is also something that can be improved, the current design eccentrically loads the door meaning wear will be accelerated.

## Pusher

### Overview

The pusher's role is to move ammunition from the storage belt through the blast doors and into the breach. To achieve this, the system requires a telescoping mechanism that can extend to seat the round and retract fully to allow the blast doors to close securely. Designing this subsystem presented several challenges, including the need to minimize binding, deflection, and mechanical failures under non-ideal conditions. The design process involved multiple iterations, each addressing key issues uncovered in previous concepts. Key objectives for the pusher subsystem include high reliability under extreme conditions, low maintenance needs, and streamlined production using accessible materials and components.

### Initial Designs

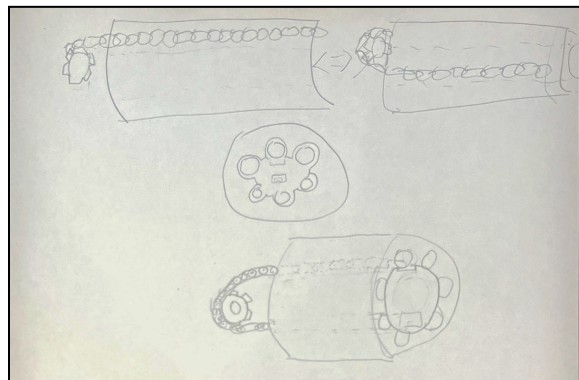


Figure 5.0, 1st conceptual design

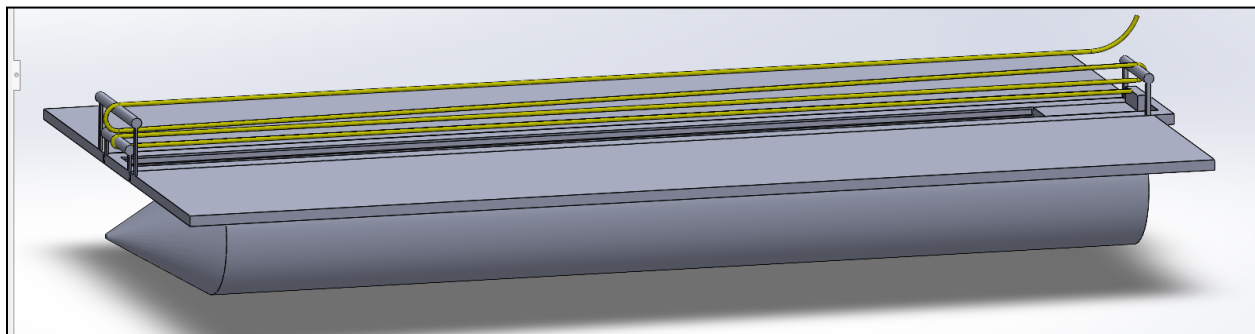


Figure 5.1, 2nd conceptual model

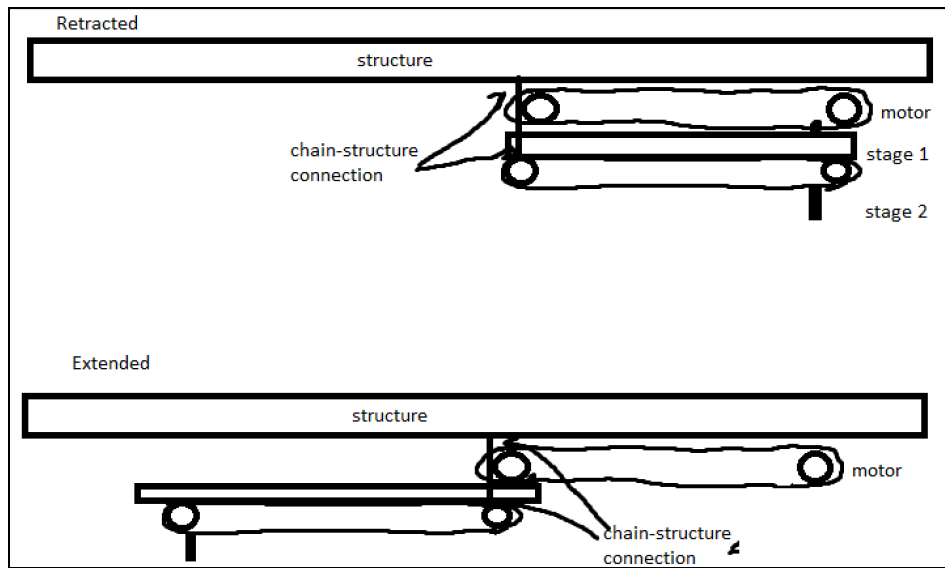


Figure 5.2, 3rd conceptual sketches

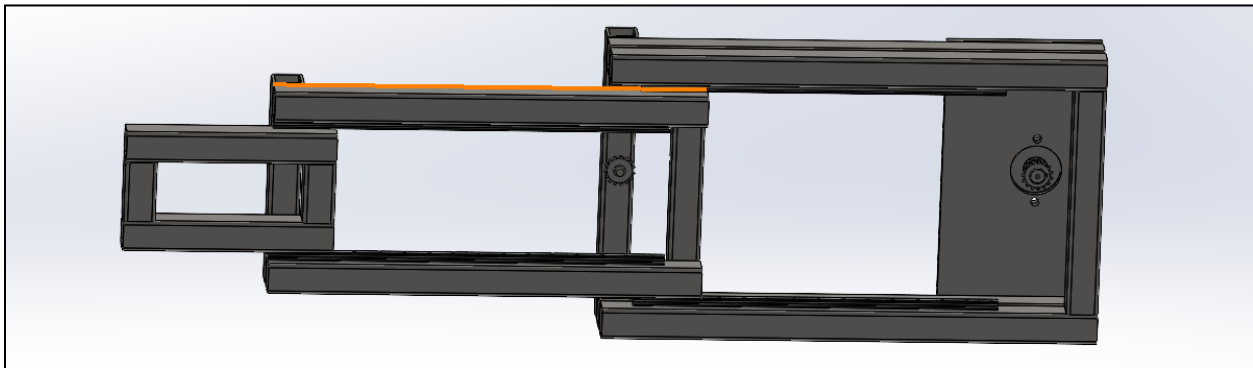


Figure 5.3, 3rd conceptual model

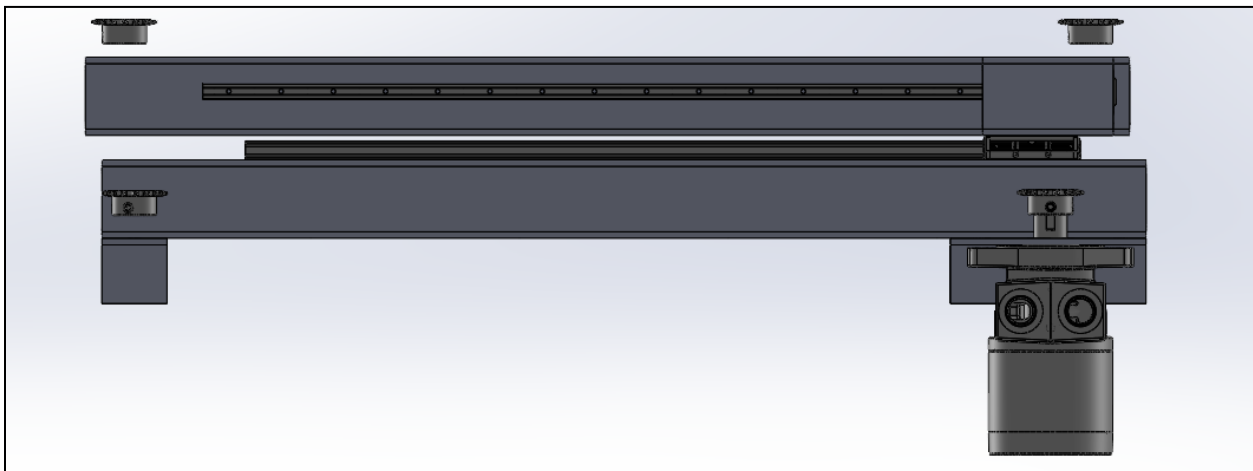


Figure 5.4, 4rd conceptual design simplified

As seen in Figure 5.0, we initially thought of using a guided chain to load the rounds, however concerns about binding and deflection led us to look into other options. This brought us to our second design as seen in Figure 5.1. This design featured two sliding extensions with one nested inside the other that would extend when a cable was spooled up. This design was then further improved upon, as seen in Figure 5.2, and refined into the model shown in Figure 5.3. This new design improves the motion system to use standard ANSI chains instead of cables as they are more reliable, and we were able to integrate the driving sprocket and system of idlers into the insides of the sliders to have a lower profile mechanism. To further minimize the size of the mechanism we essentially cut the design in half, as seen in Figure 5.4, and in doing so we are still able to have all the benefits of the previous systems while reducing the complexity and required materials.

## Structural Analysis

The pusher system underwent several design iterations to address key challenges such as binding, deflection, and overall reliability. Initial concepts included a guided chain system and a cable-driven telescoping mechanism. However, both designs were ultimately rejected due to concerns over their performance under harsh conditions. The guided chain system lacked the necessary rigidity, while the cable system introduced issues like unreliable spooling and stretching, which could lead to malfunctions. These issues highlighted the need for a more robust solution, leading to the development of the final design.

The final design incorporates a telescoping mechanism with two nested sliding extensions, powered by standard ANSI chains and driven by a hydraulic motor. This configuration eliminates the issues associated with cables while offering greater structural integrity and reliability. The internal housing of the drive sprockets and idlers reduces the mechanism's profile, maintaining a compact design without sacrificing performance. All major components were chosen with affordability, standardization, and accessibility in mind. ANSI 304 steel tubing, known for its strength and durability, was selected for the extensions, while components like the hydraulic motor, sprockets, idlers, and linear rails were sourced from McMaster-Carr to ensure that readily available, standardized parts are used.

The final design was chosen for its balanced approach, combining functionality and reliability to ensure optimal performance in challenging operational environments. The system was developed to meet the demanding conditions expected during use, offering a robust solution that ensures dependable operation even in less-than-ideal situations. This design prioritizes durability and performance while minimizing complexity, making it both practical and efficient.

To ensure the design's reliability and performance, we calculated the frictional forces acting on the pusher system to determine the necessary forces for testing. This involved analyzing the friction between various components, such as the shell, rail carriages, and sliding extensions. By using the coefficient of friction for each material and calculating the normal forces, we can estimate the total frictional forces that the system will encounter during operation. These calculations will inform the force requirements for testing the design, ensuring it can withstand the expected operational conditions.

**Friction Force**

$$f = \mu \times N$$

**Shell Friction**

$\mu = 0.4$  (*Coefficient of Friction Reference Chart*, n.d.)

$$N_{\max} = 30 [kg] \times 9.8 [m/s] = 294 [N]$$

$$f_{\text{Shell}} = 0.4 \times 294 [N] = 117.6 [N]$$

**Stage 1 Friction**

$\mu = 0.002$  (*Coefficient of Friction for Profile Rail Carriages*, n.d.)

$$m_1 = 4.202 [kg]$$

$$m_2 = 0.01149 [kg]$$

$$N_{\max} = (m_1 + m_2) [kg] \times 9.8 [m/s] \approx 46.93 [N]$$

$$f_{\text{Shell}} = 0.002 \times 46.93 [N] \approx 0.09386 [N]$$

**Stage 2 Friction**

$\mu = 0.002$  (*Coefficient of Friction for Profile Rail Carriages*, n.d.)

$$m_2 = 0.01149 [kg]$$

$$N_{\max} = m_2 [kg] \times 9.8 [m/s] \approx 5.749 [N]$$

$$f_{\text{Shell}} = 0.002 \times 5.749 [N] \approx 0.01149 [N]$$

**Force On Pusher**

$$F = f_{\text{Shell}} + f_{\text{Stage 1}} + f_{\text{Stage 2}}$$

$$F = 117.7 [N]$$

**Motor Force**

$$T_{\max} \approx 261.8 [\text{Nm}] (\text{from spec sheet})$$

$$PD_{\text{motor sprocket}} = 1.8 [\text{in}] \approx 0.04581 [\text{m}]$$

$$F_{\text{motor, min}} = 117.7 [N] = T_{\min} / (0.04581 [\text{m}] / 2)$$

$$T_{\min} \approx 2.696 [\text{Nm}]$$

**Brackets FEA**

$$N = 3$$

$$F_{\text{test}} = F_{\max} \times N = 117.7 [N] \times 3 = 353.1 [N]$$

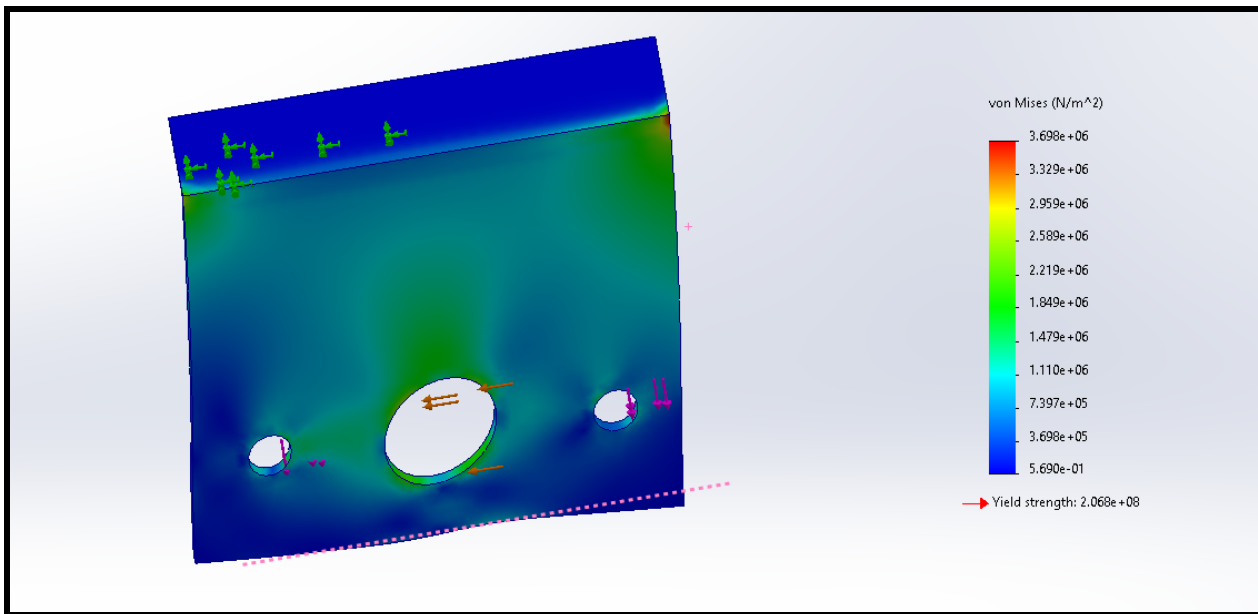


Figure 5.5: Motor Mount

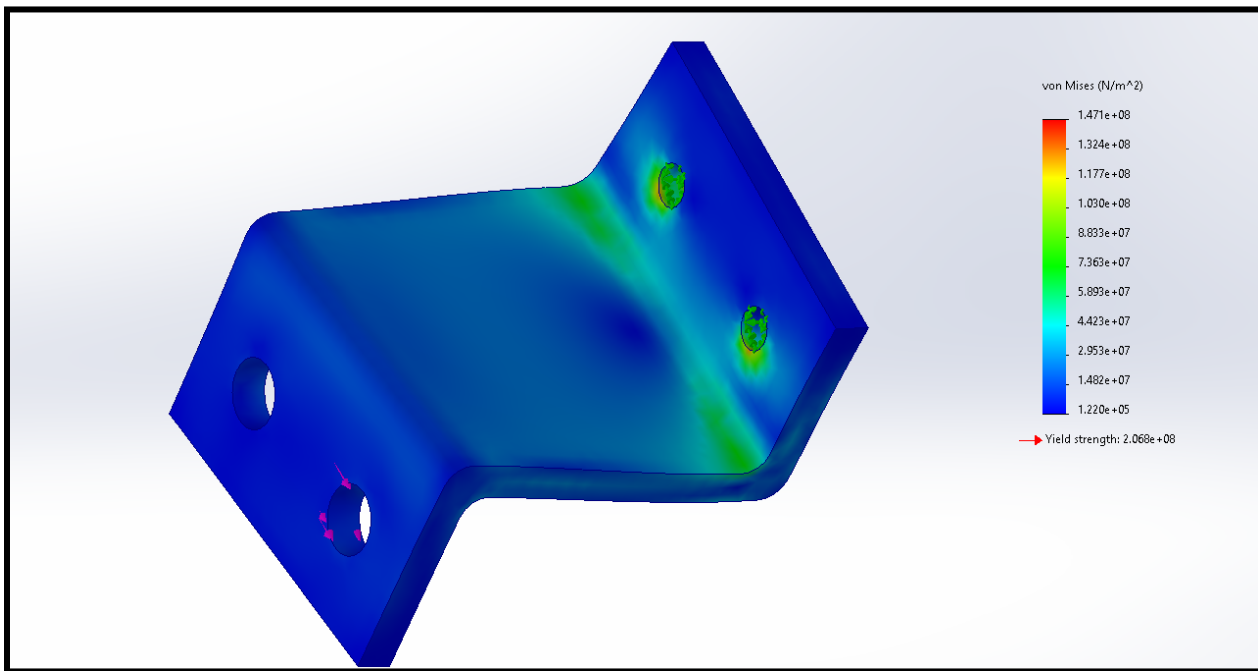


Figure 5.6: Stage 0 Chain Bracket

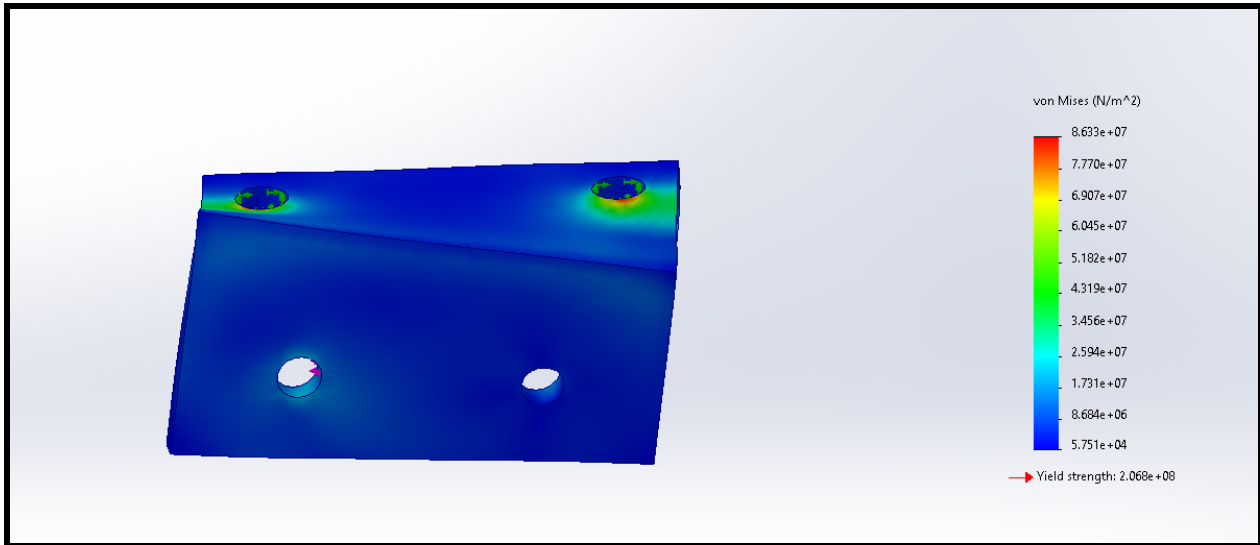


Figure 5.7: Stage 1 Chain Bracket

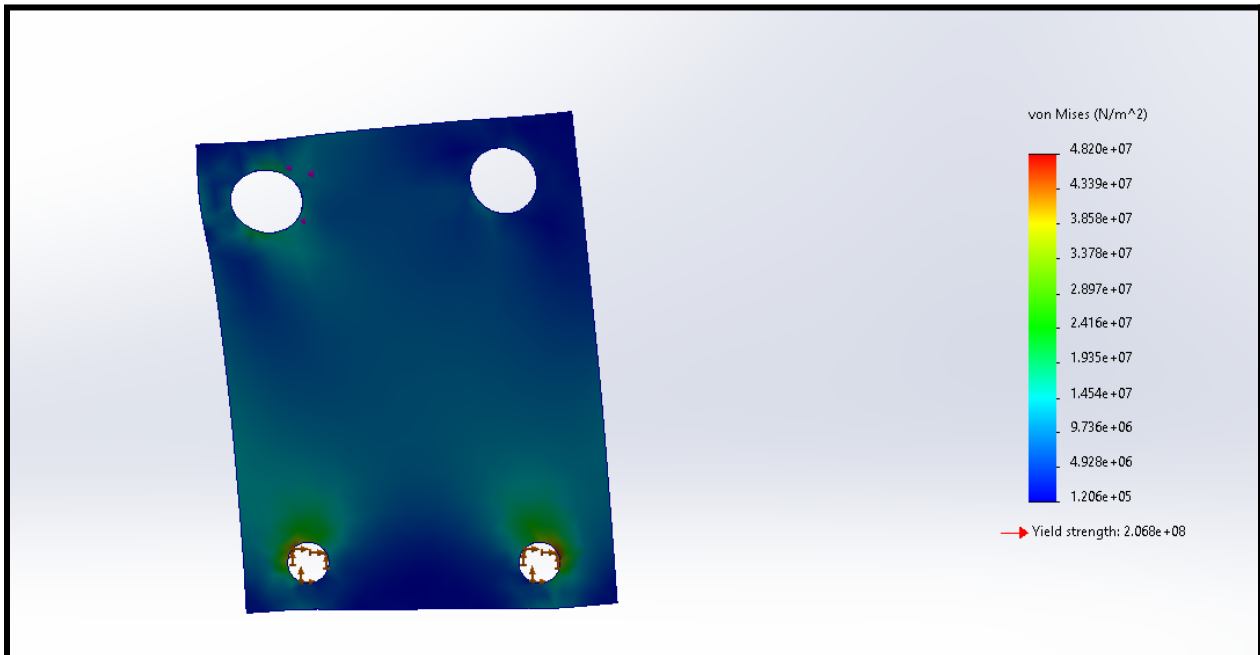


Figure 5.8: Stage 2 Chain Bracket

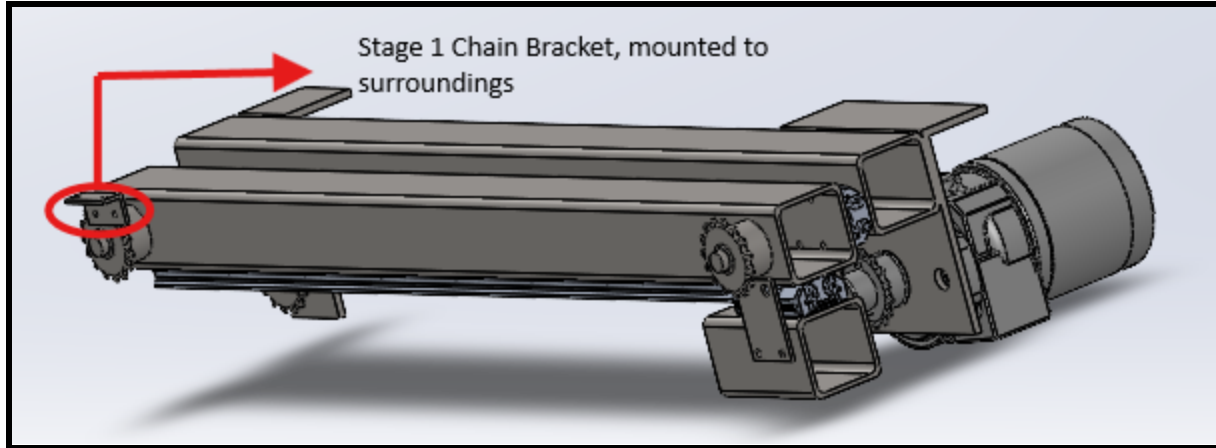


Figure 5.9: Retracted Position, No chains

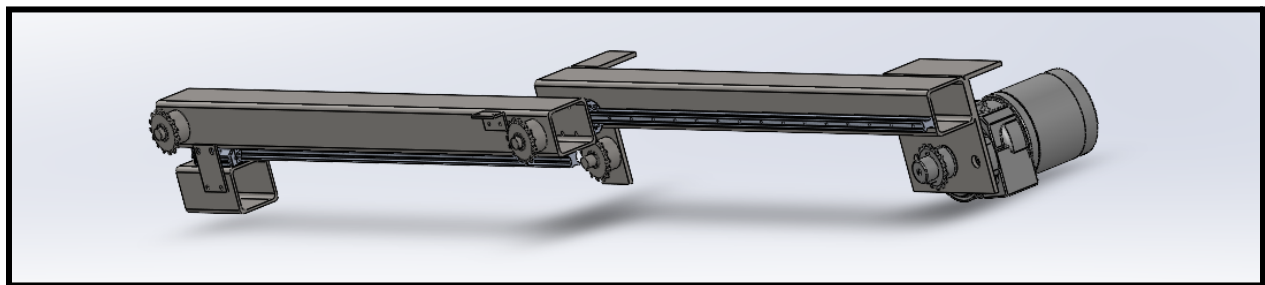


Figure 5.10: Extended Position, No chains

In terms of force calculations, friction forces acting on the pusher were calculated for various stages. The total friction force was determined to be 117.7 N, with additional considerations for the motor force required to move the pusher. Using the hydraulic motor's torque specifications, the minimum required torque was calculated to be 2.696 Nm.

Finite element analysis (FEA) was also performed on various brackets, with simulations showing that the system could withstand a force of 353.1 N, confirming the design's robustness. These simulations ensure that the design can handle the stresses it will encounter in its operating environment, further validating its reliability and performance.

## Future Improvements

The pusher subsystem is reliable and functional, but there are opportunities for refinement. One improvement involves adding a damping system, such as rubber stops or spring-loaded absorbers, to reduce impact forces when the mechanism reaches its stroke limits. This would minimize wear on components, reduce vibration, and enhance the system's durability and stability.

---

Another enhancement focuses on reducing the form factor. Optimizing the arrangement of internal components, such as the drive sprockets, idlers, and hydraulic motor, could make the mechanism more compact while maintaining its functionality. A smaller footprint would improve integration into constrained spaces, making the design more versatile.

Additionally, improving the ease of maintenance is a key area for improvement. Incorporating modular components that can be easily replaced or serviced would streamline maintenance procedures and minimize downtime. This would increase the overall reliability of the system, particularly in mission-critical environments, where quick repairs are essential.

These refinements would enhance the pusher subsystem's performance, durability, adaptability, and ease of upkeep for demanding applications.

## Full Assembly

The full assembly of the tank autoloader integrates all subsystem components into a single functional design. The ammo belt, casing, motor drive, guide rail and blast door, and the pusher have been made to work together. The motor drives the power transmission chain, which transmits a torque to the drive shaft; 64B chain with the ammo belt and casings is driven by the shaft, which positions each casing in line with the blast door. The blast door then opens, and the pusher would move the ammunition into the cannon breach, completing the autonomous loading procedure.

The modular assembly approach allowed us to design the system asynchronously, allowing for adjustments to be made for each sub-system of the autoloader. This was done to ensure a proper design process was being followed for every aspect of this project, helping us achieve the project's goal of an affordable and efficient tank autoloader system.

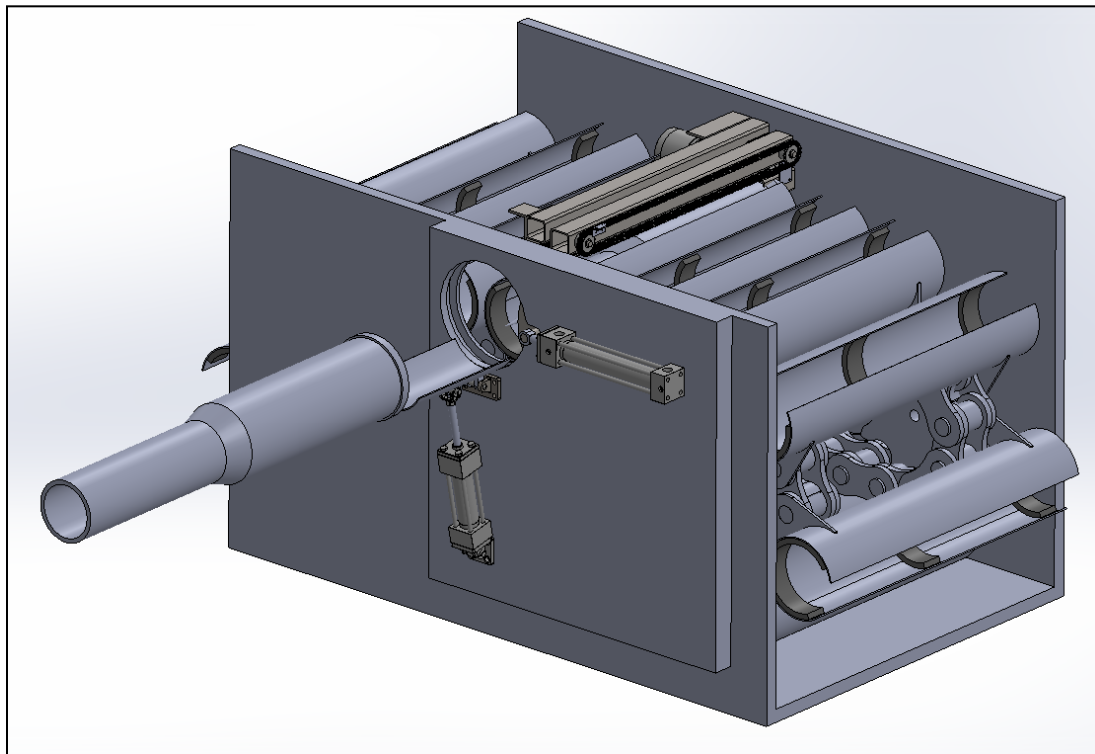


Figure 6.1: Full Assembly Model

## Conclusion

The design of the final assembled autoloader involved a number of multi-part mechanisms that must operate both cohesively and reliably with one another. Due to complexity, the project was divided into multiple subsections including: chain belt, casing, motor drive, blast-door and guide rail, and pusher. Upon extensive research, deliberation, and sketching, the initial concept designs were translated into the final finished product. The team meetings helped facilitate discussions and conceptualization on different ideas and lead to a design everyone unanimously agreed upon.

The autoloader, within the scope of the project, drew inspiration from the Leclerc and Arjun tank bustle systems. Each element involves a unique design. The ammo belt is designed to carry 16 rounds of approximately 30 kg per round using a heavy-duty chain belt system. The casing was designed to safely house a specific ammunition round, namely 120x570mm NATO shell. The motor drive was selected to provide the optimal torque with highest factor of safety while maximizing greatest torque at low speeds. The blast door and rail system, influenced by the Arjun tank bustle autoloader, provides a means to transport the individual rounds into the breach while providing protection to the crew in the event of an explosion. Lastly, the pusher was developed to transfer rounds into the breach from the casing while minimizing space occupation.

Overall, the tank autoloader project successfully integrated a range of engineering challenges and iterative designs, resulting in a weapon concept that offers significant benefits for modern tanks.

---

## References

*Coefficient of friction for profile rail carriages.* (n.d.).

*Coefficient of Friction Reference Chart.* (n.d.). Schneider & Company. Retrieved December 4, 2024, from  
<https://www.schneider-company.com/coefficient-of-friction-reference-chart/>

*M1A2 Main Battle Tank Firing Main Gun - Interior View [Film].* (n.d.).

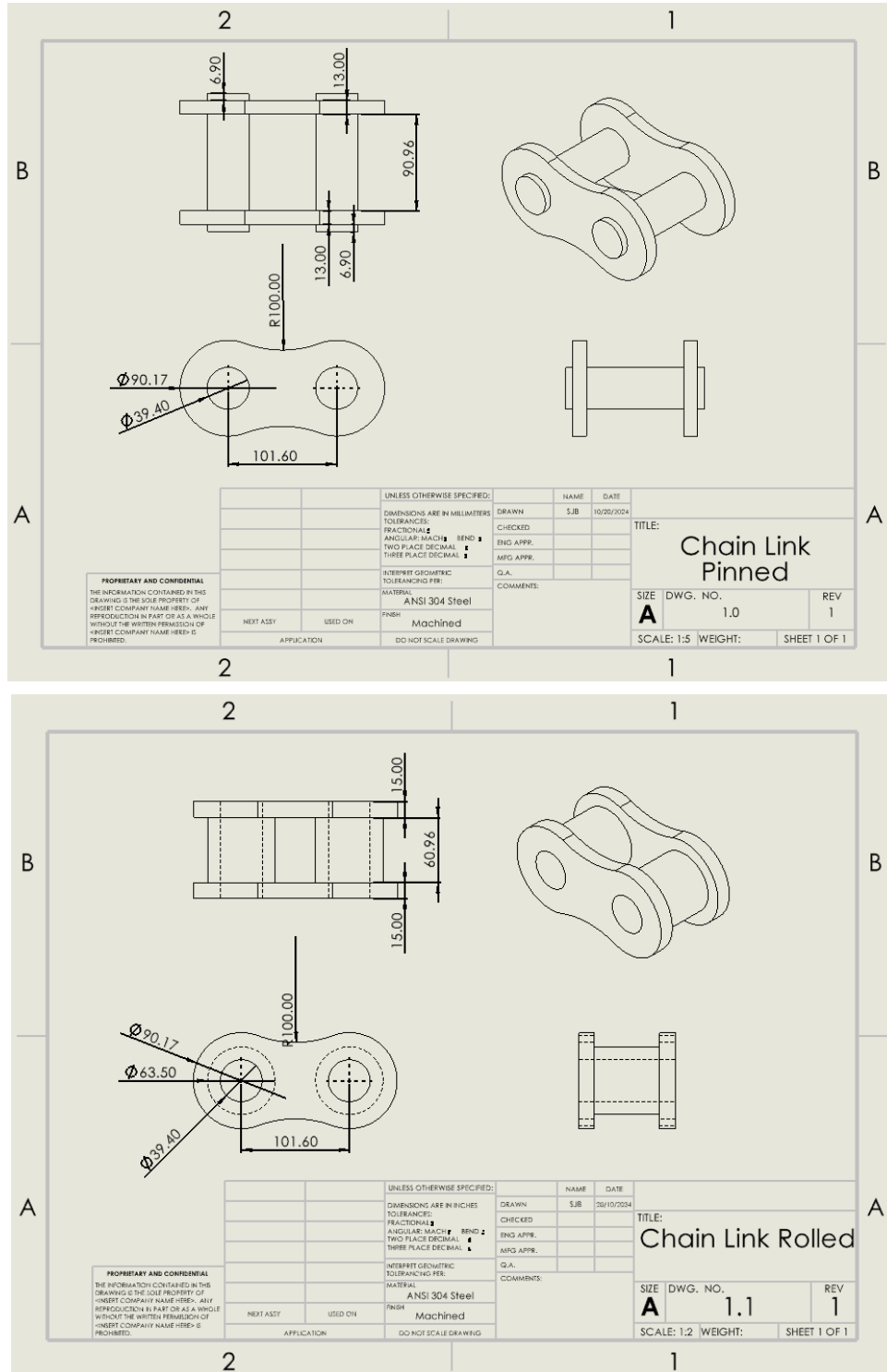
<https://www.youtube.com/watch?v=sC2ePKRvo9k>

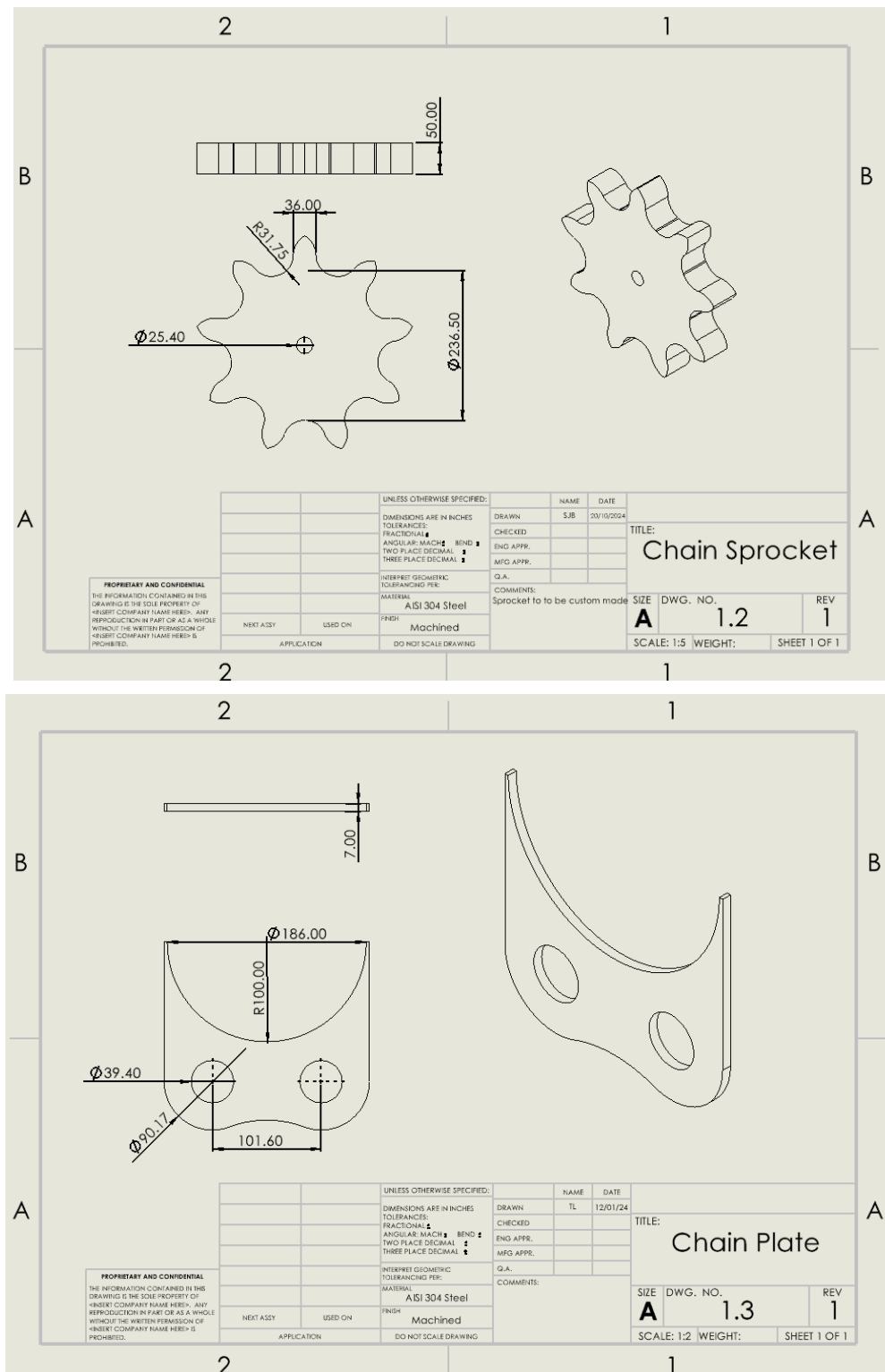
Mott, R. L., Vavrek, E. M., & Wang, J. (2017). *Machine Elements in Mechanical Design*. Pearson.

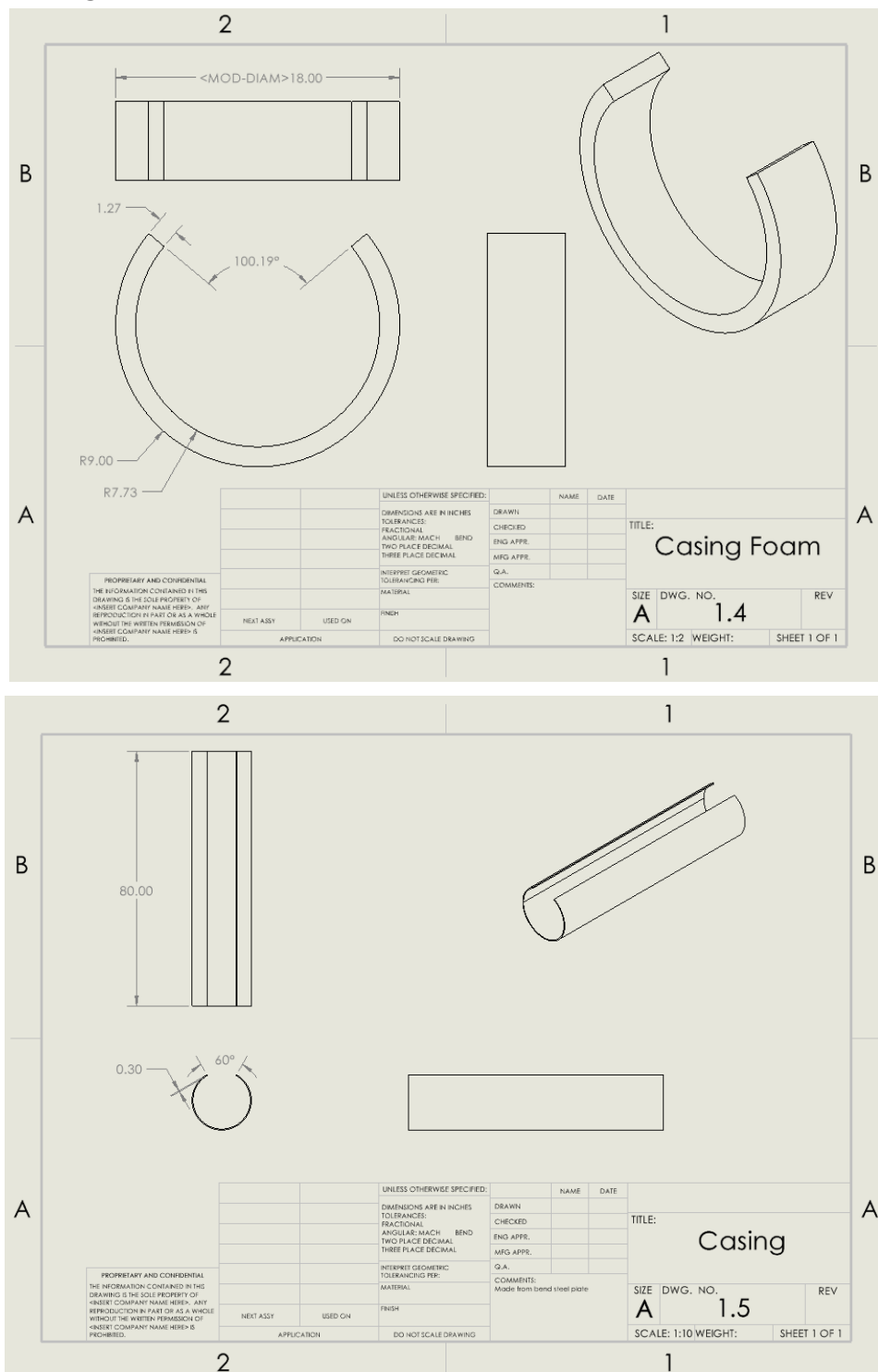
*RHEINMETALL – 120MM SMOOTHBORE.* (n.d.). Rheinmetall. Retrieved December 4, 2024, from  
<http://www.rheinmetall.com/Rheinmetall%20Group/brochure-download/Weapon-Ammmunition/B195e0423-Rheinmetall-120mm-system-house.pdf>

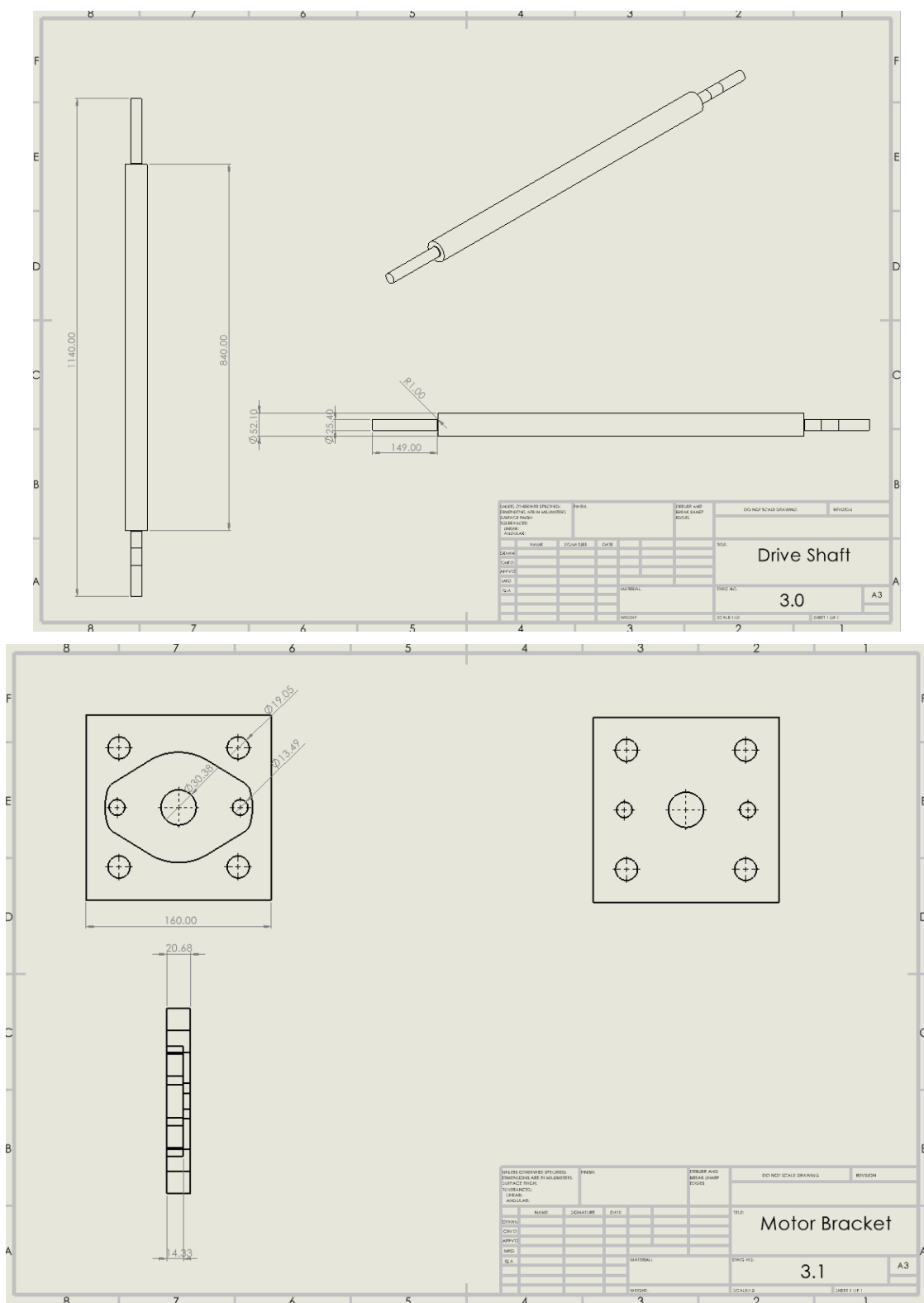
## Appendix: Engineering Drawings

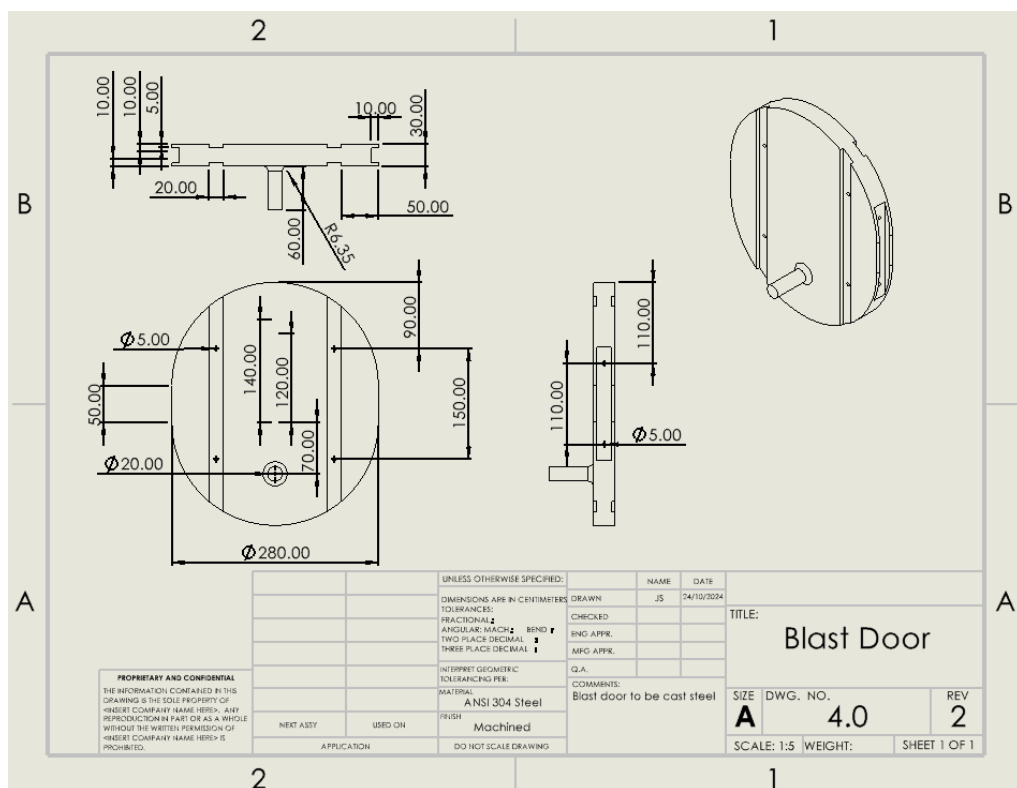
### Appendix 1: Ammo Belt

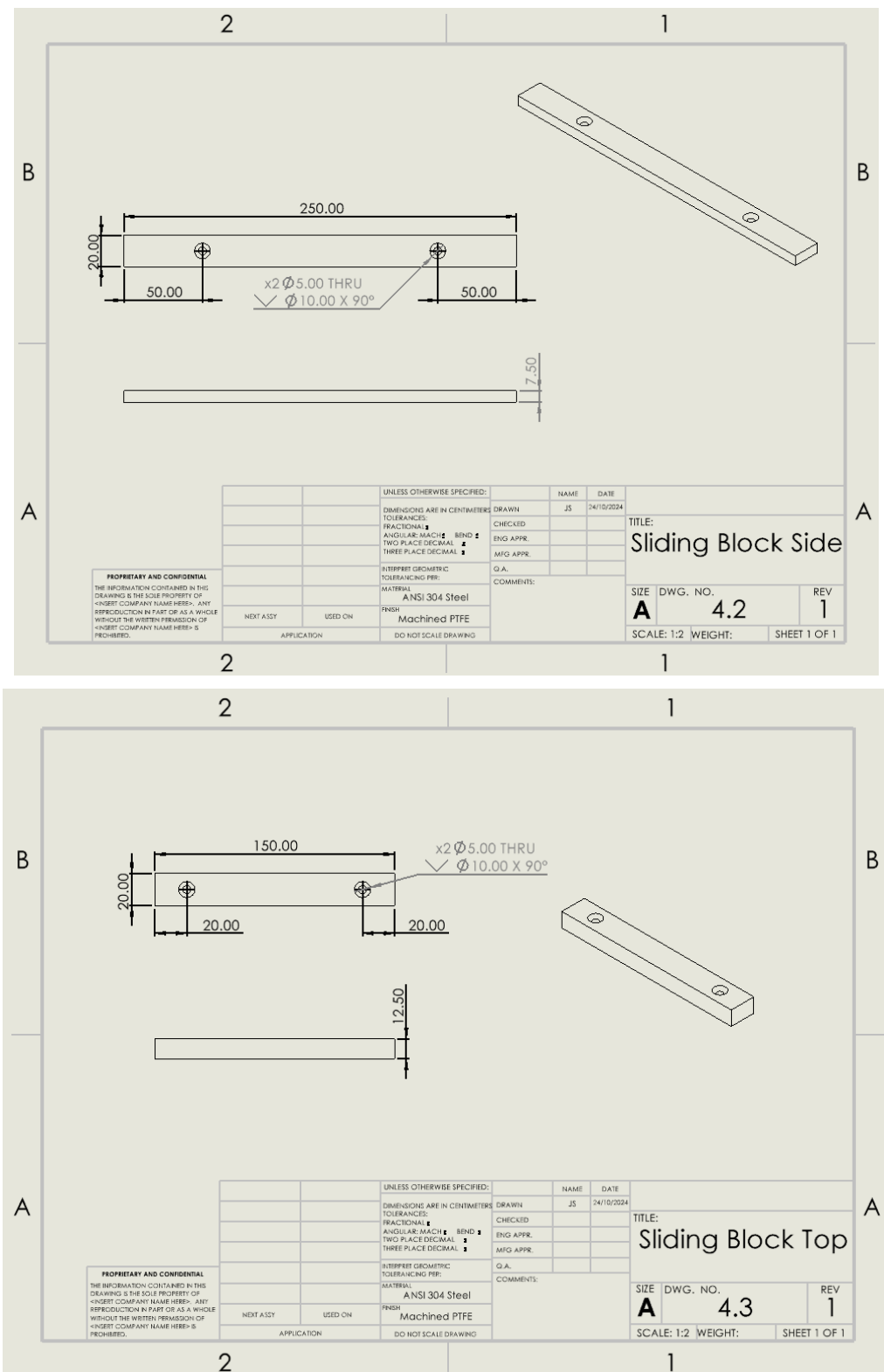


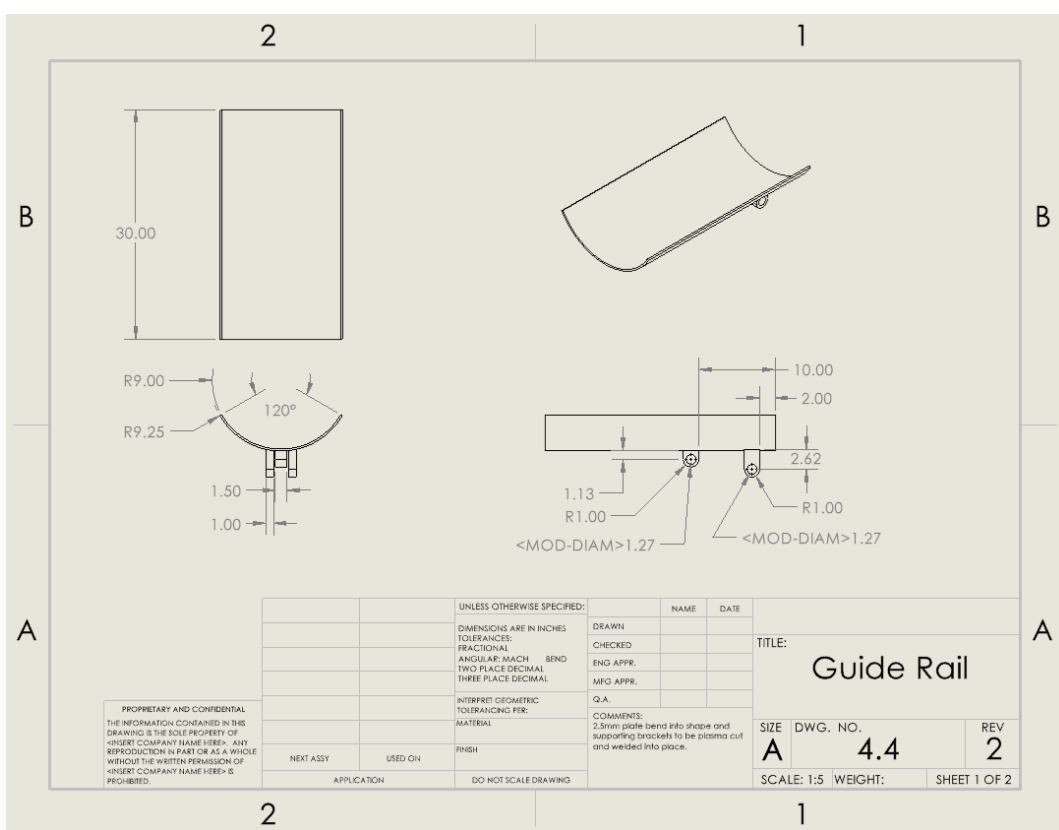
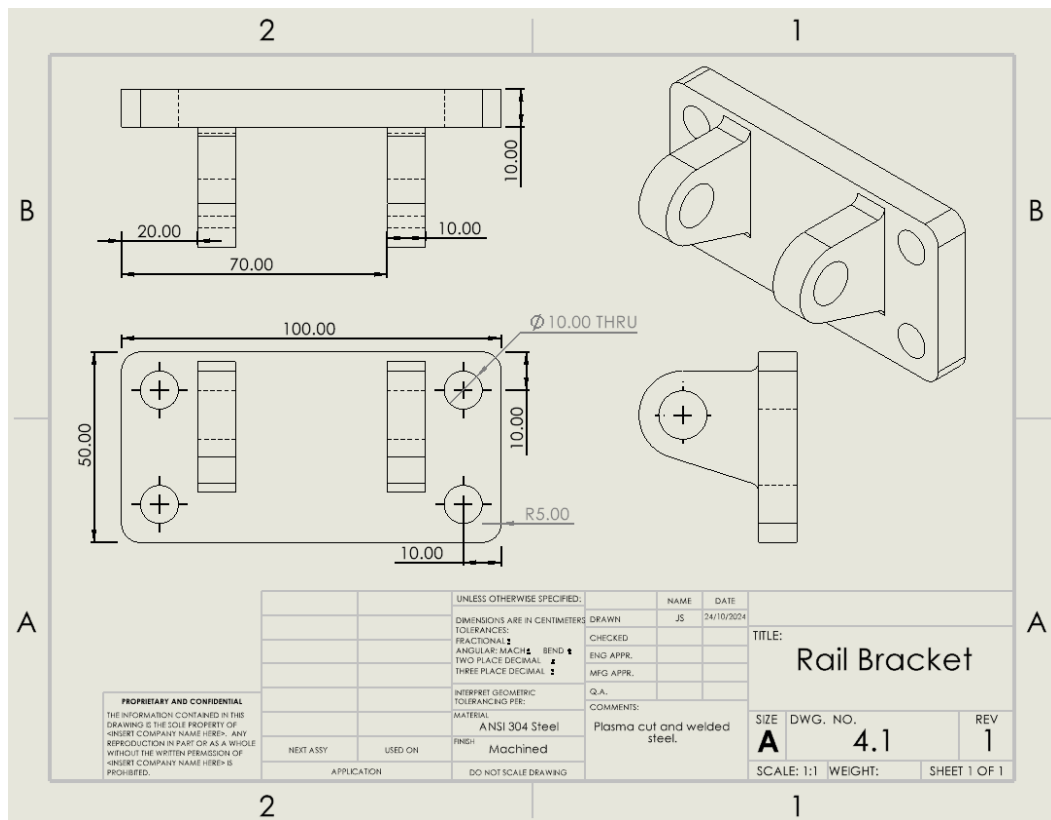


**Appendix 2: Casing**

**Appendix 3: Motor and Shaft**

**Appendix 4: Blast Door and Guide Rail**





**Appendix 5: Pusher**